

University of Montana

ScholarWorks at University of Montana

Graduate Student Theses, Dissertations, &
Professional Papers

Graduate School

2002

Assessing Landsat TM imagery for mapping and monitoring prairie dog colonies

Willard A. Gustafson
The University of Montana

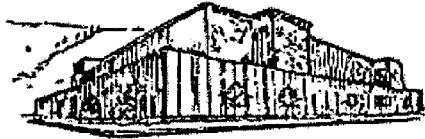
Follow this and additional works at: <https://scholarworks.umt.edu/etd>

Let us know how access to this document benefits you.

Recommended Citation

Gustafson, Willard A., "Assessing Landsat TM imagery for mapping and monitoring prairie dog colonies" (2002). *Graduate Student Theses, Dissertations, & Professional Papers*. 6570.
<https://scholarworks.umt.edu/etd/6570>

This Thesis is brought to you for free and open access by the Graduate School at ScholarWorks at University of Montana. It has been accepted for inclusion in Graduate Student Theses, Dissertations, & Professional Papers by an authorized administrator of ScholarWorks at University of Montana. For more information, please contact scholarworks@mso.umt.edu.



Maureen and Mike
MANSFIELD LIBRARY

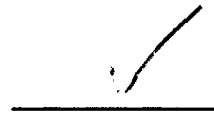
The University of

Montana

Permission is granted by the author to reproduce this material in its entirety, provided that this material is used for scholarly purposes and is properly cited in published works and reports.

****Please check "Yes" or "No" and provide signature****

Yes, I grant permission



No, I do not grant permission



Author's Signature: William A. Gustafson

Date: 8-26-2002

Any copying for commercial purposes or financial gain may be undertaken only with the author's explicit consent.

**Assessing Landsat TM Imagery
For Mapping and Monitoring
Prairie Dog Colonies**

By

Willard A. Gustafson

B.A. The University of Montana, 1997

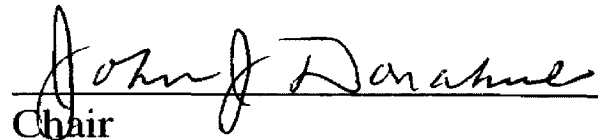
Presented in partial fulfillment of the requirements for the degree of

Master of Arts

The University of Montana

2002

Approved By:


Chair


Dean, Graduate School

8-28-02

Date

UMI Number: EP37371

All rights reserved

INFORMATION TO ALL USERS

The quality of this reproduction is dependent upon the quality of the copy submitted.

In the unlikely event that the author did not send a complete manuscript and there are missing pages, these will be noted. Also, if material had to be removed, a note will indicate the deletion.



UMI EP37371

Published by ProQuest LLC (2013). Copyright in the Dissertation held by the Author.

Microform Edition © ProQuest LLC.

All rights reserved. This work is protected against unauthorized copying under Title 17, United States Code




ProQuest LLC.
789 East Eisenhower Parkway
P.O. Box 1346
Ann Arbor, MI 48106 - 1346

ABSTRACT

Gustafson, Willard A., M.A., May 1997

Geography

Assessing Landsat TM Imagery For Mapping and Monitoring Prairie Dog Colonies

Director: John J. Donahue 

At the turn of the 20th century, prairie dog colonies (PDCs) covered between 40 and 100 million ha of the prairies of western North America (Marsh 1984, Anderson et al. 1986). However because of government eradication programs, habitat loss and more recently Sylvatic plague epidemics, PDCs have experienced a decline of nearly 98% in the last 100 years.

The goal of this research was to evaluate the effectiveness of Landsat Thematic Mapper (TM) imagery for directly mapping PDCs using a two-stage classification process. Specific objectives of this research were to: (1) determine how well PDCs can be distinguished from uncolonized prairie (UP); and (2) determine whether active PDCs can be distinguished from inactive PDCs, due to plague or other factors.

Research focused on a portion of one TM scene (Path 37/Row 27) in north central Montana (Figure 3). This study area covers part of the Charles M. Russell National Wildlife Refuge (CMR), Fort Belknap Indian Reservation, and the Bureau of Land Management's (BLM) Phillips County Resource Area. This PDCs in this area have been extensively mapped and monitored by land management agencies since the late 1970's, and is currently the site of black-footed ferret reintroductions.

My research shows that PDCs can be mapped fairly accurately using Landsat TM imagery and this methodology; however accurately distinguishing PDCs from IPDCs was not possible. The overall tendency of my classifications was to over predict PDCs and IPDCs while consistently missing the very small colonies. Although commission errors were high, a good percentage of these errors were due to confusion between active and inactive PDCs. In addition, some of the commission error may be attributed to the correct identification of active PDCs, especially on the nearly 700,000 acres of private lands, much of which has never been surveyed for PDCs. The spatial resolution of Landsat TM imagery is quite adequate for the identification of PDCs, and any higher resolution imagery would, in my opinion, create more problems than benefits.

ACKNOWLEDGEMENTS

I want to begin by thanking my parents, Roger and Karen Gustafson, for their support and love. I also want to thank my committee members: Dr. Donahue, Dr. Redmond, and Dr. Edlund. Dr. Redmond in particular for helping me stay motivated and for being a great mentor, Dr. Donahue for helping me focus my thoughts and challenging me, and Dr. Edlund for being great to work with.

I also want to express my thanks and recognition to those responsible for funding this research and making it all possible: Joe Ball of the Montana Cooperative Wildlife Research Unit, Randy Matchett of the Charles M. Russell National Wildlife Refuge, Roxanne Falice of the Bureau of Land Management, Linda Poole of The Nature Conservancy, and Minette Johnson of Defenders of Wildlife. I would like to thank Randy Matchett (again), John Grensten of the Bureau of Land Management, and Jerry Kaiser of the Bureau of Indian Affairs for providing me with their semi-annual prairie dog colony survey data. Thank you all for helping me to make it happen.

Several others who deserve thanks include Chip Fisher for keeping me on my toes and cracking that whip, Chris for helping me to ‘think’ and for all the technical advise, Melissa for always being available for questions, Dr. Steele for your consultation, and Poody for doing all that you do so well. On a personal note I would like to thank Morgan Witt for being a good friend when it counted, and Karma Cochran without whom I might never have taken this path.

TABLE OF CONTENTS

ABSTRACT	ii
ACKNOWLEDGEMENTS	iii
TABLE OF CONTENTS	iv
LIST OF FIGURES	vi
LIST OF TABLES	vii
LIST OF ABBREVIATIONS.....	viii
INTRODUCTION	1
Ecological Considerations	3
Mapping and Monitoring	4
Prairie Dog Colony Attributes	5
STUDY AREA DESCRIPTION	7
Raw Data	8
METHODOLOGY	11
Pre-Processing.....	11
Image Segmentation	13
Z-grid	17
Supervised Classification	19
Training Data	19
Classifiers	23
Terminology and Notation	23
Unweighted Euclidean Distance Classifier	24
Mean Inverse Distance Spatial Classifier	26
Product Rule	28
Accuracy Assessment	29
Leave-One-Out Cross-Validation	29
Overlay Analysis	30
RESULTS	32
Bi-Variate Classifications	32
Accuracy Assessments	37
Omission Error Analysis	38
Commission Error Analysis	39
Tri-Variate Classifications	43

Accuracy Assessments	46
DISCUSSION	48
Bi-Variate Classifications	48
Tri-Variate Classifications	49
CONCLUSIONS	50
Future Research	51
LITERATURE CITED	53
APPENDICES	56
Appendix 1. 1991 Bi-variate Data.	56
Appendix 2. 1993 Bi-variate Data.	57
Appendix 3. 1993 Tri-variate Data	58
Appendix 4. 1995 Bi-variate Data	59
Appendix 5. 1995 Tri-variate Data	60

LIST OF FIGURES

Figure 1. Black-Tailed Prairie Dog.	1
Figure 2. Black-Footed Ferret.	4
Figure 3. Example of a prairie dog colony in a Landsat TM false color composite image using bands 4(red), 5(green), and 3(blue). Surveyed boundaries are shown in black. Note the apparently unsurveyed PDC in the left central portion of the image.	6
Figure 4. False color composite using bands 4, 5, and 3 showing extent of Landsat TM scene P37/R27 with the study area boundary shown in red.	8
Figure 5. Study Area for the Assessment of Landsat TM Imagery for Mapping and Monitoring Prairie Dog Colonies.	10
Figure 6. False color composite image map (bands 4, 5, 3) of the study area. White areas identify unsuitable habitats.	13
Figure 7. An example of how the ISODATA clustering algorithm divides spectral space. Reproduced with permission from Jensen, 1996.	15
Figure 8. A comparison of raw and segmented images showing prairie dog colonies with surveyed boundaries shown in black.	17
Figure 9. Distribution of Training Regions Used for the 1991 Bi-variate Classification.	22
Figure 10. 1991 Bi-variate Classification Results.....	34
Figure 11. 1993 Bi-variate Classification Results.....	35
Figure 12. 1995 Bi-variate Classification Results.....	36
Figure 13. 1993 Bi-variate Commission Analysis Results.....	41
Figure 14. 1995 Bi-variate Commission Analysis Results.....	42
Figure 15. 1993 Tri-variate Classification Results.....	44
Figure 16. 1995 Tri-variate Classification Results.....	45

LIST OF TABLES

Table 1. Relationships between land stewardship and the number of acres of PDCs observed vs. predicted for the bi-variate classifications.	33
Table 2: Leave-one-out cross-validation statistics for the bi-variate classifications.	37
Table 3: Results of the bi-variate classifications overlay analyses showing the proportions of each error type and correctly classified areas.	38
Table 4: Results of the omission error analyses for the bi-variate classifications identifying the number and acreages of colonies that were missed or partially predicted/missed.	39
Table 5: Results of the commission error analysis comparing PDC commission and IPDCs.	40
Table 6: Relationship between the surveyed and predicted areas of each covertype for the tri-variate classifications.	43
Table 7: Leave-one-out cross-validation statistics for the tri-variate classifications.	47
Table 8: Results of the tri-variate classifications overlay analyses.	48

LIST OF ABBREVIATIONS

BIA	Bureau of Indian Affairs
BLM	Bureau of Land Management
BOR	Bureau of Reclamation
CMR	Charles M. Russell National Wildlife Refuge
DD	Difference Density
DEM	Digital Elevation Model
GIS	Geographic Information Systems
GPS	Global Positioning Systems
IPDC	Inactive Prairie Dog Colonies
ISODATA	Iterative Self-Organizing Data Analysis Technique
k -NN	" k " Nearest Neighbors
MCV	Mean Covariate Vector
MDM	Minimum Distance to Means Classifier
MID	Mean Inverse Distance classifier
MMU	Minimum Mapping Unit
MNDVI	Modified Normalized Difference Vegetation Index
PDC	Prairie Dog Colonies
SED	Spectral Euclidean Distance
SR	Spectral Response
TM	Thematic Mapper
TR	Training Regions
UED	Unweighted Euclidean Distance Classifier
UP	Uncolonized Prairie
USFWS	United States Fish and Wildlife Service
WSAL	Wildlife Spatial Analysis Lab

Introduction

Prairie dogs live in densely populated colonies across the Great Plains from Canada to Mexico. They are not really "dogs" but are, in fact, closely related to herbivorous ground squirrels. During their explorations Lewis and Clark dubbed them prairie "dogs", because of the animals' distinctive "bark-like" alarm call. At the turn of the 20th century, prairie dog colonies (PDC) covered between 40 and 100 million ha of the prairies of western North America (Marsh 1984, Anderson et al., 1986). The largest single prairie dog colony on record, in Texas, was 100 miles wide and 250 miles long and contained an estimated 400 million prairie dogs (Foster, 1990).



Figure 1. Black-Tailed Prairie Dog.

Because prairie dogs keep vegetation closely cropped in and around their colonies (Clippinger, 1989) they were assumed to be responsible for the overgrazing of many western rangelands. So when Merriam estimated, in 1902, that prairie dogs reduced range productivity by as much as 50-75%, state and federal governments, looking to

increase forage production for cattle, established programs to eradicate prairie dogs. These programs were highly successful, and by 1960 the total range of prairie dogs had been reduced to approximately 600,000 ha (Marsh, 1984). By conservative measures this represents a decline of around 98% in less than 100 years. Some of these eradication programs persisted until the late 1980's despite modern research showing that the level of competition between prairie dogs and cattle was only 4-7% (Uresk and Paulson, 1988), meaning it would take approximately 300 prairie dogs to eat as much as one cow and calf (Miller et al., 1994).

Although the decline of PDCs is primarily a result of these eradication programs, other contributing factors to their decline include the spread of sylvatic plague (*Yersinia pestis*) and the conversion of native prairie to agricultural production. Sylvatic plague is currently thought to be the single greatest threat to the health of PDCs, "no other diseases of prairie dogs have the potential to cause epizootics of higher mortality to prairie dog populations (Miller, et al., 1994)." All species of prairie dogs are susceptible to plague, and colonies are often totally eradicated by the disease. The plague is spread through fleas carried on predators such as coyotes, badgers, and ferrets who visit many colonies in their search for food. Currently there is no known method of protecting PDCs from the plague. However recent efforts suggest that upon detection of plague, burrows should be dusted with insecticide to kill infected fleas and limit the spread of plague. Predator control is also used to prevent plague from spreading to adjacent colonies (Miller et al., 1994).

Ecological Considerations

More than 100 wildlife species depend at least to some extent on PDCs for habitat (Clark et al., 1989; Sharps and Uresk, 1990), and several species, such as the mountain plover (*Chadarius montanus*), and black-footed ferret (*Mustela nigripes*), have evolved very close relationships with prairie dogs. The disappearance, fragmentation, and resulting isolation of PDCs are responsible for the decline of these two species, as well as the decline in the overall biodiversity of the prairie ecosystem (Miller et al., 1994).

Black-footed ferrets, widely recognized as one of the most endangered species in North America, depend entirely on PDCs for food and shelter. These ferrets were almost extinct in the 1980's except for a small population near Meteetse, Wyoming. When, in 1985, this population almost perished from canine distemper, the surviving individuals were captured and placed in a captive-breeding program. This breeding program was successful, and in 1989 plans were initiated to reintroduce black-footed ferrets back into the wild (Oldemeyer, 1993). Because black-footed ferrets depend entirely upon PDCs for their sustenance, knowledge of PDC locations, sizes, and relative health is of utmost importance. However, because of the spread of sylvatic plague, continued expansion of agricultural production, and the sheer vastness of the Great Plains, the number, size, and whereabouts of healthy PDCs have proven difficult to inventory, and expensive to track.



Figure 2. Black-Footed Ferret.

Mapping and Monitoring

The methods for mapping PDCs have evolved significantly over the years. Early surveying efforts relied on visual estimation of colony size and location on topographic maps. With the goal of increasing their accuracies, researchers in the 1970's began experimenting with black and white aerial photography, and later color infrared photography for PDC mapping. Unfortunately, these efforts proved to be “inadequate” and too expensive (Biggens et al., 1993).

Currently, ground surveys using global positioning systems (GPS) are the most common way of mapping and monitoring PDCs. While planimetrically accurate, GPS surveys are very labor intensive, and depend upon the subjective judgments of each individual surveyor. Consequently, this method is limited by manpower, time, and consistency, and, as such, may not be suitable for broad-scale applications.

The emergence of geographic information systems (GIS) has facilitated the development of new computer models focused mainly on the evaluation of the extent and

quality of prairie dog habitat. Some examples include the Habitat Suitability Index (Clipinger, 1989) and the more recent habitat models by Reading (1997), and Proctor (1998). These models employed multivariate statistical analysis to predict the most suitable habitat types based on slope, aspect, soil type and vegetation.

The goal of this research was to evaluate the effectiveness of Landsat Thematic Mapper (TM) imagery for directly mapping PDCs using a two-stage classification process. I chose Landsat TM imagery because it is readily available, relatively cheap, and because a preliminary unsupervised classification of a Landsat TM image showed a strong association between a spectral classes and prairie dog colony boundaries (Redmond pers. comm., 2001). Specific objectives of this research were to: (1) determine how well PDCs can be distinguished from uncolonized prairie (UP); and (2) determine whether active PDCs can be distinguished from inactive PDCs, due to plague or other factors.

Prairie Dog Colony Attributes

My research depends upon the capacity of the Landsat TM satellite to remotely sense differences between UP and PDCs, and more subtly, between active PDCs and inactive PDCs (IPDC). These differences include the presence of unvegetated burrows, the shortness of the vegetation within the colonies, and the altered composition of that vegetation. Biomass is significantly lower on PDCs, averaging 95g/m^2 compared to 190g/m^2 on the surrounding UP. There is also a corresponding shift in vegetation composition with greater than 95% of PDC biomass being composed of forbs, whereas forbs make up less than 15% of the biomass on adjacent UP (Coppock et al., 1989).

Research suggests that upon initial abandonment of PDCs (1-2 yr) there is a 32% to 36% increase in biomass, primarily stemming from an increase in grasses. This results in a slight decrease in the relative abundance of forbs and an increase in the relative abundance of grasses (Cid et al., 1991), and is the result of selective foraging by prairie dogs. Prairie dog colonies are ordinarily one of the first areas to green-up in springtime, which in north central Montana usually occurs in late March or early April (Randy Matchett pers. comm., 2001). They also stand out well in late summer against the drier prairie grasses due to the abundance of forbs and the immature growth stage of grasses on PDCs. To take advantage of these seasonal high contrasts I selected cloud free images recorded during early spring or late summer.

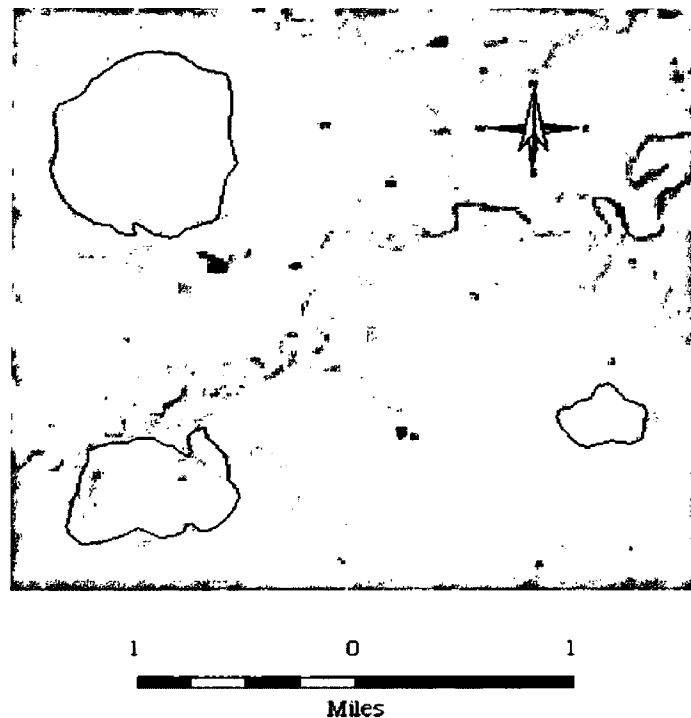


Figure 3. Example of a prairie dog colony in a Landsat TM false color composite image using bands 4(red), 5(green), and 3(blue). Surveyed boundaries are shown in black. Note the apparently unsurveyed PDC in the left central portion of the image.

Study Area Description

Research focused on a portion of one TM scene (Path 37/Row 27) in north central Montana (Fig. 3). The study area covers part of the Charles M. Russell National Wildlife Refuge (CMR), Fort Belknap Indian Reservation, and the Bureau of Land Management's (BLM) Phillips County Resource Area. This region incorporates a wide range of physiographies. The CMR portion is dominated by the Missouri River Breaks, which consist of deep valleys, ranging from 500 to 1000 feet below the surrounding plains and having steep forested walls and mixed grass and sagebrush floors. The Fort Belknap and Phillips County portions are open rolling prairie dissected by intermittent streams and deep coulees. The dominant vegetation in this portion of the study area consists of grasses and sagebrush.

Across much of this area the PDCs have been mapped and their status monitored by the United States Fish and Wildlife Service (USFWS), Bureau of Indian Affairs (BIA), and the BLM since the late 1970's, and throughout the plague epidemic, which began in 1992. Portions of this area have also been studied extensively through habitat modeling (Proctor, 1998, Reading and Matchett, 1997). Because of the overall quality and number of the PDCs in this region, it has been identified as a nationally significant area for prairie dogs and species dependent upon them (Proctor, 1998). In addition, the area has been targeted for black-footed ferret reintroductions, which have been taking place on several healthy colonies throughout the region. The importance of this area for the protection of PDCs and associated species, as well as the wealth of historical survey data, makes it an optimum study area for my research.

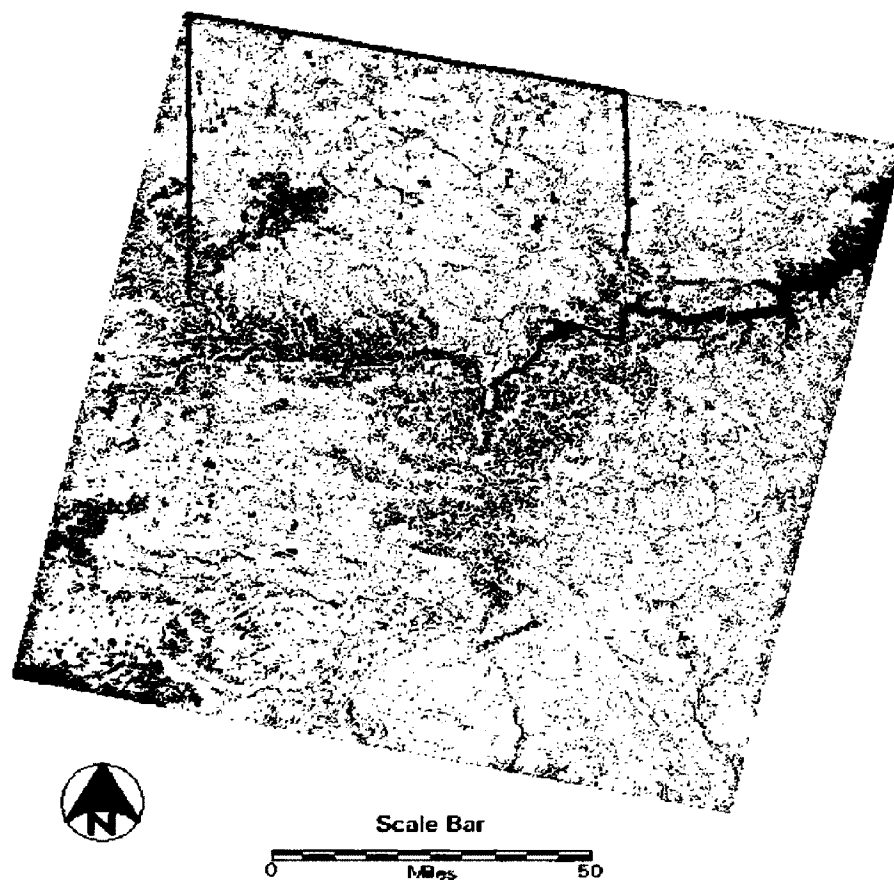


Figure 4. False color composite using bands 4, 5, and 3 showing extent of Landsat TM scene P37/R27 with the study area boundary shown in red.

Raw Data

In addition to a complete set of the survey data, I also obtained Landsat TM imagery for three dates coinciding approximately with the cycle of plague infestation, and the dates of the survey data. The first date, 1991, represents pre-plague conditions and will be used in conjunction with the 1988 survey data. From the second and third dates, 1993 and 1995, I will attempt to measure declining conditions one and four years after the plague infestation initially occurred.

Landsat TM imagery is collected by satellites, specifically Landsat 5 and Landsat 7, which carry sensors that record electromagnetic reflectance from the earth in several

wavelengths or bands. Landsat TM imagery has a 30-meter spatial resolution, which means that each pixel represents a 30 X 30 meter area on the ground. For each pixel, data for 7 bands, TM1-TM7, are collected. Each pixel's value for each band is stored using 8 bits, allowing the data values to range between 0 and 255. Thus each band is essentially a grayscale image made up of 256 distinct shades of gray; zero recording no reflectance and 255 recording maximum reflectance or saturation. Multiple bands may be viewed in color by assigning one band to each color gun, red, green, or blue, on a computer monitor producing what is known as a false color composite. For visual inspection, I generally assigned TM4 to the red gun, TM5 to the green gun, and TM3 to the blue gun.

Some other data that were used during the classification and subsequent analyses include a digital elevation model (DEM), an ownership layer; other layers such as hydrography, roads, and political boundaries were used primarily for cartographic production.

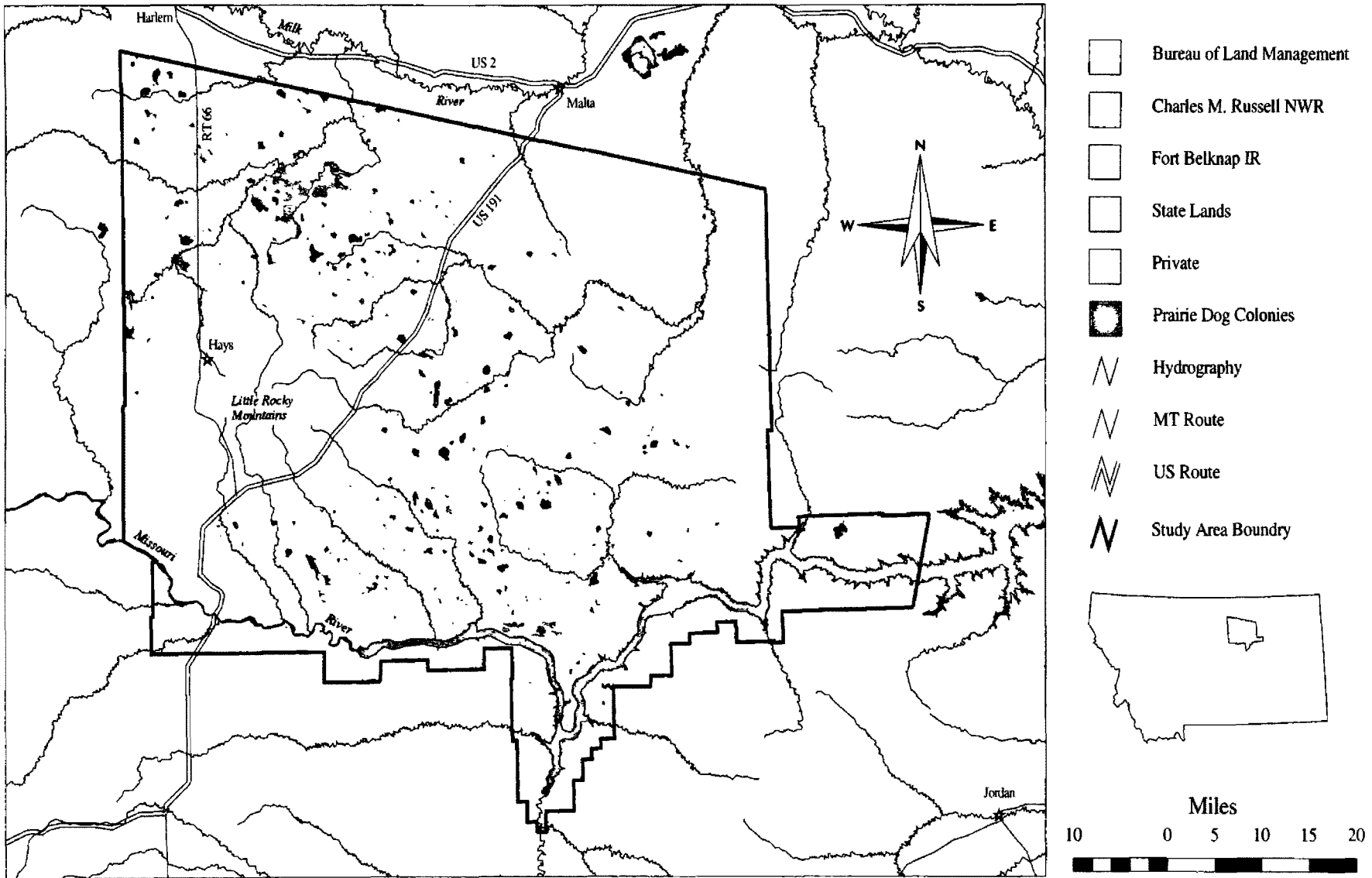


Figure 5. Study Area for the Assessment of Landsat TM Imagery for Mapping and Monitoring Prairie Dog Colonies.

Methodology

My classification methodology consisted of two major stages: image segmentation and supervised classification. During image segmentation the image was first run through a clustering algorithm that divided it into groups of spectrally similar pixels, i.e. an unsupervised classification. These similar pixels were then clumped together spatially creating a spectrally and spatially segmented image of relatively homogenous regions (Ma et al., 2001). These regions potentially represent distinct patches of vegetation or landcover, i.e. forest stands, meadows, rock outcrops, and especially, in this case, prairie dog colonies.

The second stage of the classification involved labeling each of these patches or regions with its correct coertype using supervised classification techniques. Supervised classification relies on areas of known coertype, i.e. a training sample, to assign labels to the rest of the regions created during the image segmentation. This two-stage method combining unsupervised and supervised classification techniques has been shown to be an effective way of classifying landcover (Ma et al., 2000; Steele et al., in press). It is also a way to improve the usefulness of ancillary data by pre-grouping the range of unique spectral features in the image prior to supervised classification (Wilkie and Finn, 1996).

Pre-Processing

After clipping the TM images to my study area boundary, I excluded, or masked out, as much of the non-potential PDC area as possible. The areas that were masked out included croplands, steep slopes, the Little Rocky Mountains, and water. Cropland masks

were created for each image by digitizing their boundaries on-screen. Because PDCs very rarely occur on slopes greater than 25% (Reading, and Matchett, 1997), I masked out these areas using a slope grid derived from a 30m DEM. I also used a DEM to create a mask for the Little Rocky Mountains by eliminating all elevations greater than 1200m. Because water absorbs virtually all light in TM band 7, areas that have very low reflectance values in this band, i.e. below 20, were likely to be water.

By masking out areas unsuitable for PDCs I hoped to avoid some of the confusion associated with having one very broad class, UP, and two much narrower classes, PDC and IPDC. Furthermore, by limiting the broader class only to areas that could potentially be colonized, i.e. narrowing the broad range of acceptable covertypes, the differences between UP, PDC, and IPDC were accentuated. An additional but minor benefit of the masking was a reduction in the number of pixels/regions to be classified.

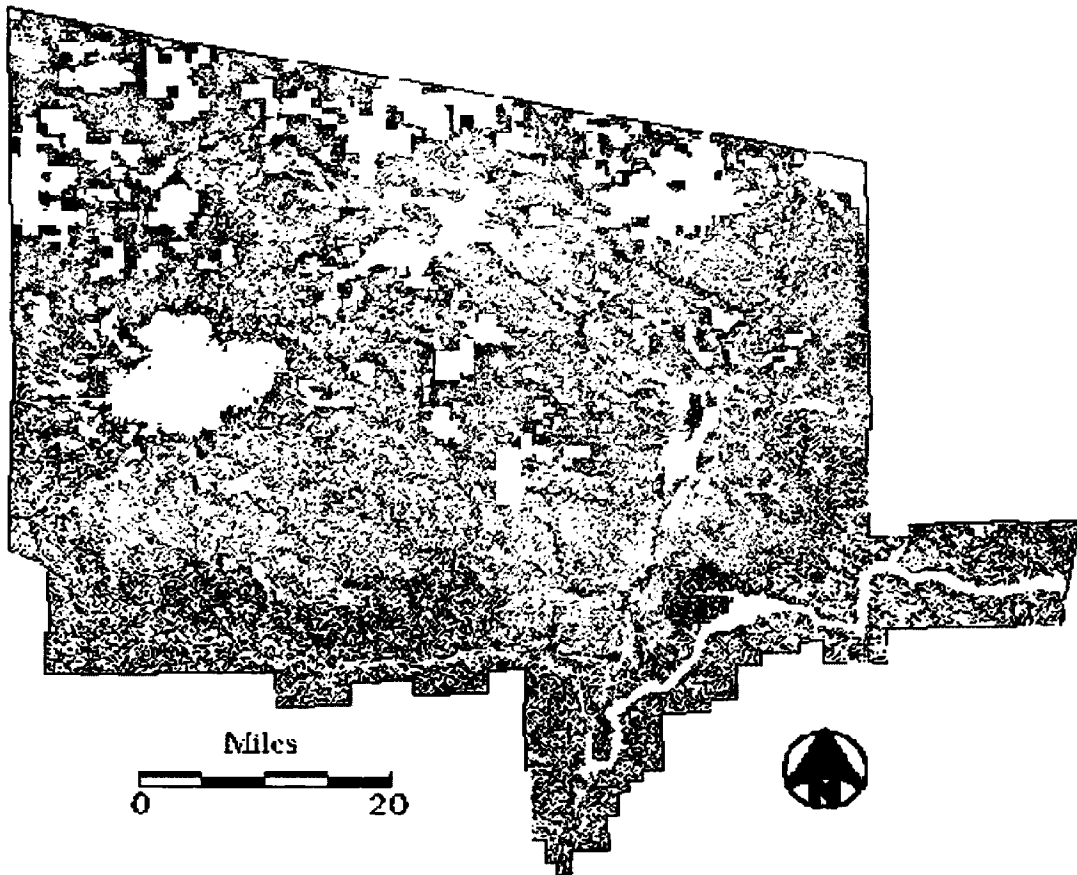


Figure 6. False color composite image map (bands 4, 5, 3) of the study area. White areas identify unsuitable habitats.

Image Segmentation

The unsupervised classification phase of the image segmentation stage was performed using the ISODATA clustering algorithm available in Erdas Imagine 8.4 using Landsat TM bands 1-7. ISODATA stands for Iterative Self-Organizing Data Analysis Technique; it iteratively performs complete classifications of the image and recalculates cluster statistics many times (Erdas Field Guide, 1997). Some advantages of the ISODATA algorithm are: (1) it is not geographically biased because it is iterative instead of single pass; (2) it is highly successful at finding natural patterns in the data; and (3) it makes no difference where the initial cluster means are located so long as enough

iterations are performed (Erdas, 1997). I used a custom program that incorporates the ISODATA algorithm and allows the user to specify the number of clusters, a convergence threshold, and the maximum number of iterations per run. The convergence threshold was the maximum percentage of pixels that remained unchanged between iterations, i.e. if there is virtually no change between iterations ISODATA stops. Initially the means of the clusters were arbitrarily determined, and an iteration was run. In subsequent iterations, the cluster means were recalculated based on the previous classification results, causing them to shift position in spectral space (Figure 7). These new cluster means then provided the basis for the next iteration. This process continued until either the convergence threshold or the maximum number of iterations was reached.

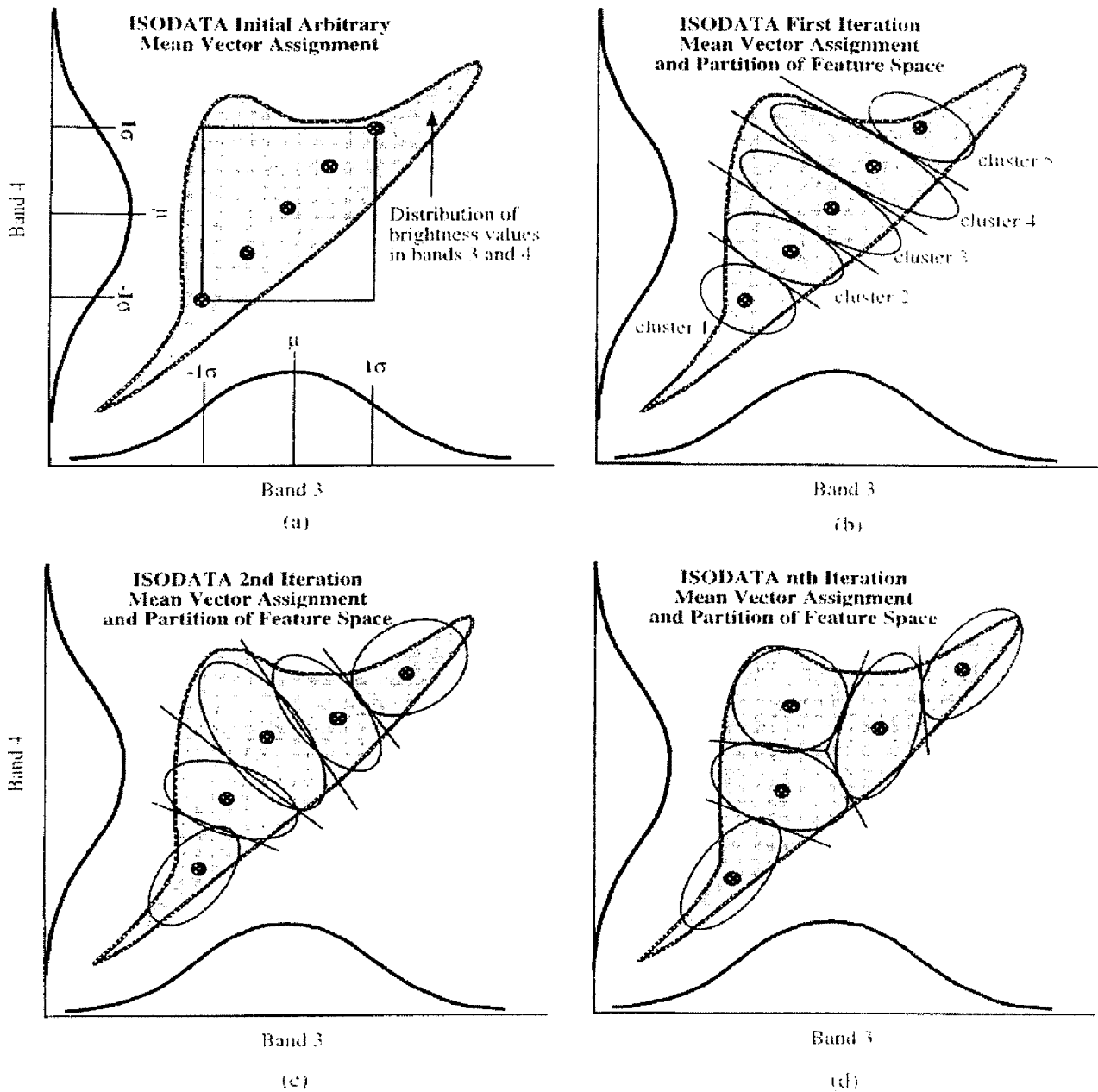


Figure 7. An example of how the ISODATA clustering algorithm divides spectral space. Reproduced with permission from Jensen, 1996.

Initially the ISODATA routine was run seven times, each one producing between 13 and 23 spectral classes. The classes were then combined to produce a set of 119 initial spectral classes. These spectral classes were then manually analyzed. Some classes were

split and others merged based on their spectral similarity, the number of pixels belonging to the class, and whether or not they were a potential PDC class. I focused mainly on splitting the larger potential PDC classes into smaller classes to discern the subtle differences between PDC and IPDC. Merging of spectral classes is easily done, however the splitting of classes was more complicated. The classes to be split were extracted from the image and re-classified using ISODATA into multiple classes, and then merged back into the original set of spectral classes. I settled on a final set of 150 spectral classes and used a minimum distance to means classifier (see unweighted Euclidean distance classification on page 24) to complete the unsupervised classification of the image.

When the unsupervised classification was complete the 150-class image was spatially segmented using custom software built around the M86 merge algorithm (Barsness, 1998) to group pixels of like spectral classes into regions. The M86 algorithm initially identifies the boundaries between spectral classes, and then merges pixels together using two major decision rules, a region size threshold, and a spectral similarity threshold. The regional size threshold is the maximum size at which a region will not be merged further preventing very large regions from dominating the landscape. The spectral similarity threshold is the maximum difference between spectral groups that is allowable when merging. This prevents very dissimilar spectral types from being combined regardless of their spatial extent.

After the merge, the mean region size was just over 1 acre and the smallest region size was .22 acres. In order to filter out the scattered small regions and standardize the minimum mapping unit (MMU) to 1 acre between the classifications, I merged all regions less than an acre in size into their surrounding covertype.

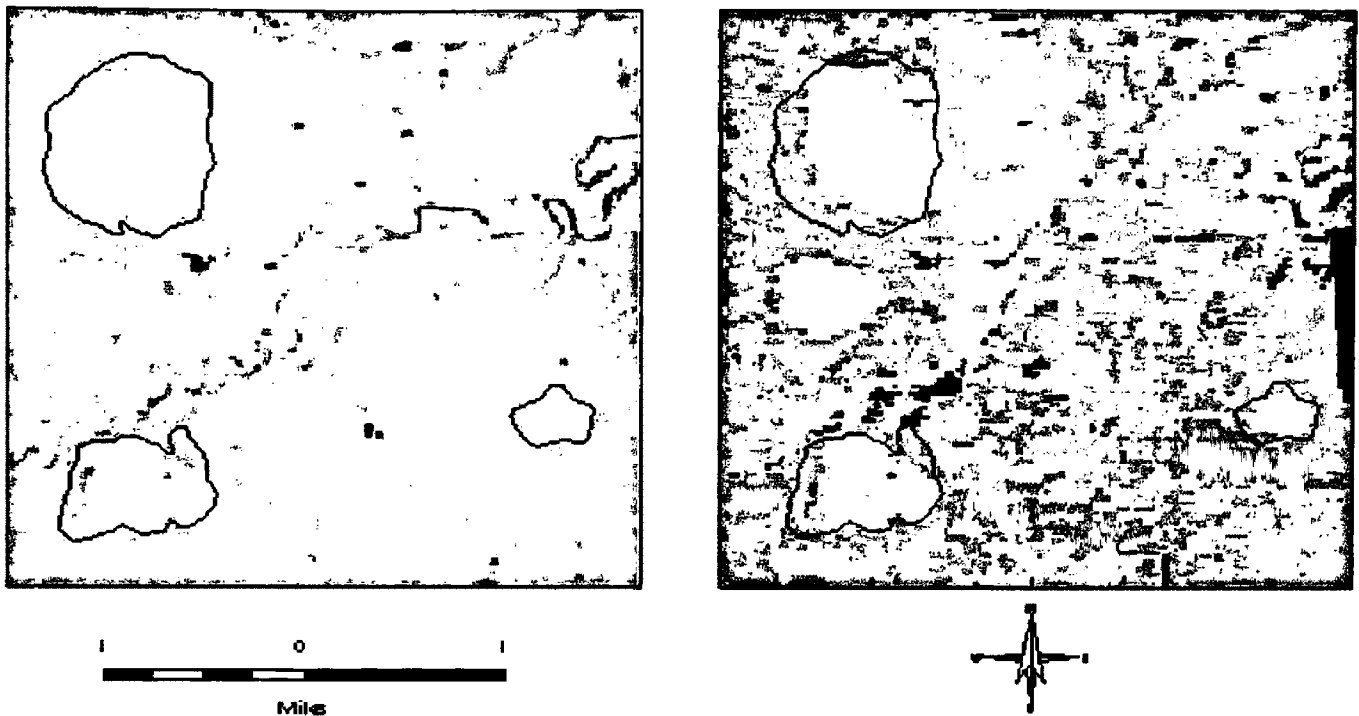


Figure 8. A comparison of raw and segmented images showing prairie dog colonies with surveyed boundaries shown in black.

Z-grid

Upon completion of the merge, the image was prepared for the supervised classification. This preparation resulted in an ArcInfo grid called the zone grid or z-grid. The z-grid's Info database housed the attributes for each region in the grid. These attributes included a unique regional identification number, a pixel count, the mean value for each TM band, 1-7, and the mode spectral class value. Modified Normalized Difference Vegetation Index (MNDVI), a measure of biomass production adapted from Nemani et al. (1993), was then added to the database. It was calculated using the formula:

$$MNDVI = \left(\left(\frac{TM4 - TM3}{TM4 + TM3} \right) \left(\frac{256}{TM5 + 1} \right) 100 \right)$$

Four topographic attributes were calculated from a 30-meter DEM and added as well. These attributes were elevation, aspect, slope, and a solar insolation index. Elevation was recorded in meters, aspect was divided into eight 45-degree wedges (1-8) with the first value mapped to north and ascending clockwise, and slope was measured in degrees. The solar insolation index was designed by Brian Steele and was calculated using slope, aspect, and the following algorithm (Steele, unpublished):

$$ins = \left(slp \left(\cos \left(\left(\frac{(((asp - 1)45) + 135)}{360} \right) 6.2832 \right) \right) \right)$$

Setting slope aside for now, the transformation maps the southwest aspect to 1 and the northeast aspect to -1. All other aspects fall in between: northwest and southeast go to 0, north and east go to -.707, and south and west go to +.707. These values are then multiplied by slope to produce the solar insolation index.

At this juncture each region in the z-grid had the following attributes: value, count, spectral-class (from the image segmentation), mean values for TM Bands 1-7, mean MNDVI, mean elevation, mean slope, majority aspect, and mean solar insolation. Nine of these variables were used directly as inputs into the supervised classification: TM Bands 1-7, MNDVI, and solar insolation. I excluded slope, aspect and elevation as direct inputs to the classification because I had already partially accounted for slope and

elevation during pre-processing, and by using solar insolation, I already had a topographic attribute that provided beneficial results in landcover classifications.

Supervised Classification

Once the z-grid was prepared, a supervised classification was used to assign a coertype label to each region. Supervised classification initially uses a training sample to generate statistics about the represented coertypes, and then uses these statistics to predict a region's coertype. Coertype labels were assigned to the unknown regions based on an evaluation of coertypes for the most similar samples. Because supervised classification depends on knowledge of land cover for training, careful selection of the training data was very important.

Training Data

Because of the importance of training data, its selection must be undertaken with great care. The main reason stems from geographic variation within coertype classes. Geographic variation occurs within a single coertype due to differences in soil types, moisture, topography, and other factors. Thus a single land cover type can have a different spectral response from one part of the study area to another. One way to mitigate the effects of geographic variation is through the use of stratified random sampling when selecting the training samples (Wilke, and Finn, 1996). Stratified random sampling divides a population into internally homogeneous sub-populations (strata) based on *a priori* knowledge about the population. In this case the survey data, (*a priori* knowledge) was used to stratify the training samples by coertypes. These samples were

then used to generate specific information about each covertype to increase the precision of the estimates about the population (Congalton, 1988).

I initially drew together my training sample by using a random number generator and ArcInfo to generate 50,000 points. These 50,000 points were then overlaid on the z-grids for each classification and any duplicate points falling within a region were eliminated. The remaining points were then edited further to remove any falling within uncharacteristic, mixed, or atypical regions so as to prevent them from adversely affecting the final classification (Wilkie and Finn, 1996). After editing, I had a set of more than 30,000 points randomly distributed across the study area. The attribute data for each sampled region, i.e. a region with a point falling within its boundaries, was then added to the Info database of that point. From this master sample set I then randomly selected the training samples required for each classification.

According to Lillesand and Keifer (1994) each covertype must have at least $n + 1$ samples, where n is the number of variables (spectral bands, etc). In practice, however, the usual minimum number of training regions ranges from $10n$ to $100n$. Wilkie and Finn (1996) suggest additionally that $50n$ pure pixels are required to estimate the spectral response (SR) for each land cover class. My analysis uses nine variables (TM1-7, MNDVI, and solar insolation) suggesting that, according to Lillesand and Keifer, I need between 90 and 900 samples from each covertype and at least 450, according to Wilkie and Finn, from each to estimate the SR of the classes. However, because these recommendations failed to address the need for proportionality in a stratified sampling scheme, I decided upon a compromise between proportional sample size and the minimum sample to effectively estimate SR within each class. I set the number of PDC

training regions at a minimum of 500, slightly above what was needed for estimation of SR, limited the UP training sample size to 5000, and set the IPDC training sample size at a minimum of 200. These numbers corresponded to a computationally efficient sample size that conformed as much as possible to the guidelines outlined in Lillesand and Keifer (1994) and Wilkie and Finn (1996), while keeping within the spirit of a proportional sample. The relatively high proportion of sampled to unsampled regions in the PDC and inactive PDC covertypes, as compared with the UP covertype is appropriate because of their small area, and their need for adequate representation (Congalton, 1988). An added benefit of keeping the sample size relatively small is that it permits land management agencies to collect field data and perform PDC classifications semi-annually without having to survey every known PDC. In essence the model, if successful, will provide more efficient options to agencies responsible for monitoring PDC populations.

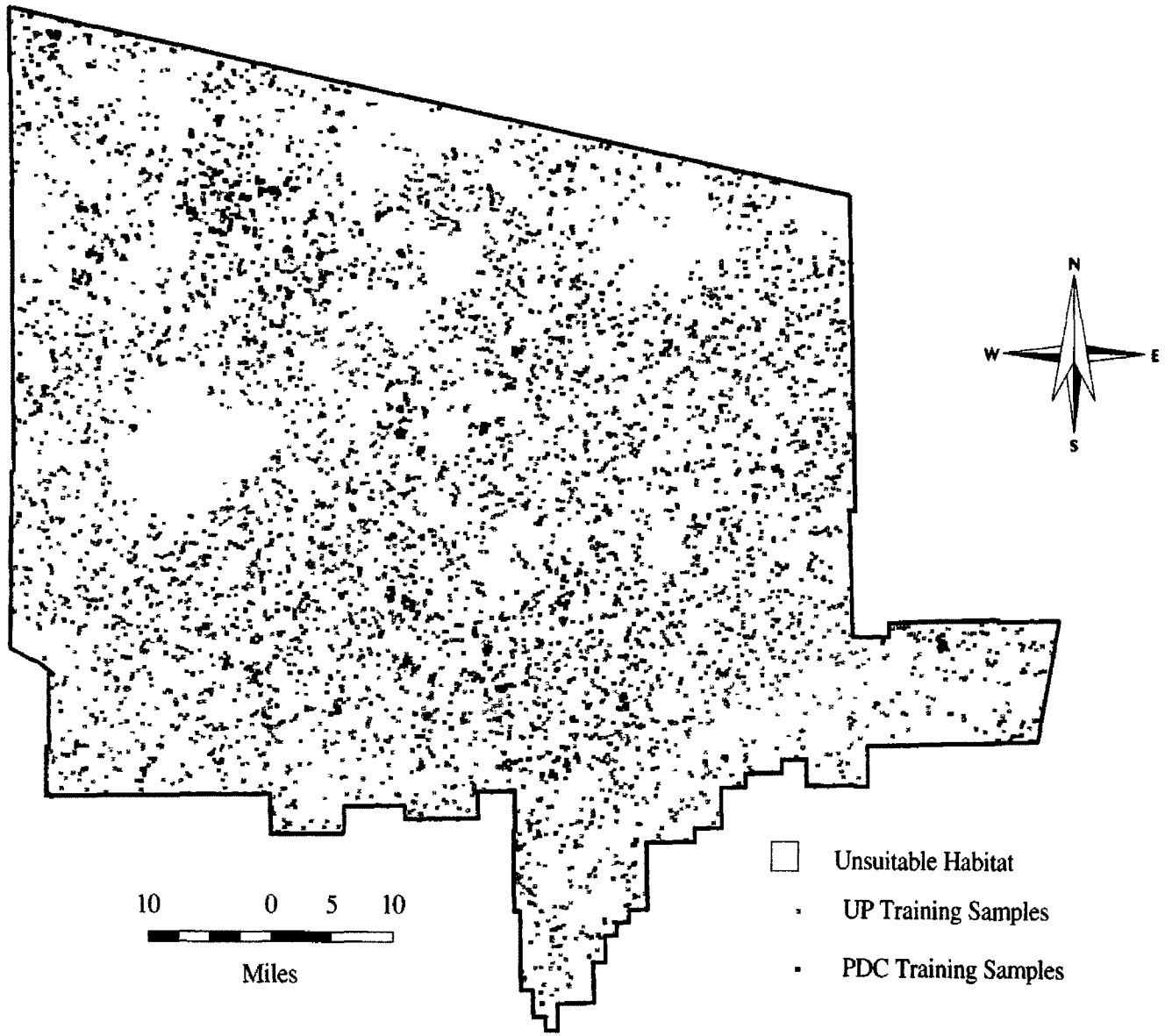


Figure 9. Distribution of Training Regions Used for the 1991 Bi-variate Classification.

Classifiers

Supervised classification can be conducted using a variety of classification algorithms. I used a combination of unweighted Euclidean distance (UED) and Mean Inverse Distance (MID) classifiers. I selected this combination classifier because it yielded consistently accurate coertype results for all 3 dates, and was relatively simple conceptually in comparison to other classifiers. I will focus on the UED and MID classifiers and how, using the product rule, the two individual classifiers, UED and MID, were combined to produce a single more accurate coertype classifier.

Terminology and Notation

Following Steele and Patterson (2001) suppose that a training sample $x = \{x_1, \dots, x_n\}$ has been collected by sampling a population P consisting of n coertypes, C_1, \dots, C_n . The i^{th} observation is denoted by $x_i = (t_i, c_i, z_i)$, where t_i is the mean covariate vector (MCV) (explained in detail on page 24), c_i is a coertype label, and z_i is a pair of location coordinates. For my study, P is the set of regions created by the image segmentation, z_i is the location of the centroid of the i^{th} sampled region, c_i is the coertype label at z_i , and t_i represents the remotely sensed and terrain variables observed at z_i . For an unclassified region x_0 , t_0 and z_0 are known, but the coertype c_0 is unknown. The posterior probability that x_0 belongs to coertype C_c , given t_0 and z_0 is denoted by $P_g(x_0) = P(c_0 = c | x_0)$. A classifier can be viewed as an estimator of $P_1(x_0), \dots, P_n(x_0)$ that assigns x_0 to the group with the largest posterior probability estimate (Steele, 2000). The posterior probability $P_g^{UED}(x_0)$ produced by the unweighted Euclidean distance classifier is the percentage of the k -nearest neighbors belonging to C_c , where the distances between x_0

and the training observations x_1, \dots, x_n are the Euclidean distances from t_0 to the covariate vectors t_1, \dots, t_n . The posterior probability $P_g^{MID}(x_0)$ produced by the mean inverse distance classifier is the probability that the covertype C_c is going to occur at location x_0 given the relative proximity's of the other training samples.

Unweighted Euclidean Distance Classifier

The unweighted Euclidean distance (UED) classifier, similar to the Minimum Distance to Means classifier (MDM) (Lillesand and Kiefer, 1987, and Jensen, 1996), used spectral Euclidean distance (SED) as a measure of how similar the covertypes of unlabeled regions were to the covertypes of the training regions. SED is the distance between two n-dimensional vectors, or MCVs, in spectral space computed in n-dimensions where n is the number of bands" (Erdas, 1997). The differences between the unlabeled regions and the training samples for each covertype, i.e. their SEDs, were calculated by comparing the MCVs of the unlabeled regions and the MCVs for each covertype represented by the training samples. A MCV is defined by the values of each variable either from the training samples of a covertype class, or from each unlabeled region. The smaller the SED between an unlabeled region's MCV and a covertypes MCV, the closer the similarity of the two and, thus, the more likely that the unlabeled region should be labeled as that covertype. In a traditional MDM classification the SEDs are calculated between each unlabeled regions MCV and the average MCV for each covertype using the following formula (Wilkie and Finn, 1996):

$$T_x U_y = \sqrt{\sum_{n=1}^b (T_{xn} - U_{yn})^2}$$

Where $T_x U_y$ is the Euclidean distance between training region x 's MCV and unclassified region y 's MCV, T_{xn} is the mean variable n value for training region x , U_{yn} is the mean variable n value for unknown region y , and b is the number of variables in the classification. The coertype producing the smallest SED, i.e. the MCV most similar to that of the unclassified region, labels that region.

The UED classifier I used is very similar to the MDM classifier with one major exception. While the minimum distance to means classifier compares each coertype's average MCV, calculated using all the training samples in each coertype, with each unclassified region's MCV; the UED classifier compares each individual training regions' MCV with those of each unclassified region. The training regions are then sorted from closest to farthest and the first " k " nearest neighbors (k -NN) according to spectral Euclidean distance are selected. These k -NN training regions are then used to calculate the mode coertype, which then is assigned to the region in question.

Historically, MDM classifications use a k -NN size of one, thus, only the single nearest neighbor to an unlabeled region classified its coertype. However, experimentation with different k -NN sizes can lead to higher classification accuracies because every training data set has an optimum neighborhood size at which the classification is most accurate (Steele and Redmond, 2001). To determine the optimum k -NN size for my classification I employed a simple looping algorithm to iteratively test all neighborhood sizes from 1 to 100. The k -NN size producing the highest accuracies,

i.e. the “optimum” k -NN size, was then used to perform the final classification. The “ k ” nearest neighbors were selected from the sorted list of training regions, and the covertype that occurred most often in the k -NN, i.e. the mode covertype, classified the region. If a tie were to occur, the neighborhood size was slowly expanded, until a modal covertype resulted.

Mean Inverse Distance Spatial Classifier

The Mean Inverse Distance (MID) spatial classifier was used to determine the spatial configuration of training observations around each unclassified region (Steele and Patterson, 2001). This was accomplished by calculating the mean inverse distance between the centroid of an unclassified region and the centroids of all the training regions for each covertype. The resulting patterns were then used to identify areas whose spatial characteristics closely matched those of the each covertype (Steele and Redmond, 2001).

The MID classifier measures spatial Euclidean distances, in meters, as opposed to spectral Euclidean distance, which is measured by the UED classifier. Mean inverse distance, $\delta_g^{MID}(z_0)$, between a region with location z_0 and all training regions with covertype G_g is defined as:

$$\delta_g^{MID}(z_0) = \frac{1}{n_g} \sum_{i \in I_g} \delta_i^E(z_0)^{-q},$$

Where I_g denotes a set of indices for the group G_g training regions with i being the i^{th} training region in the set of I_g , $\delta_i^E(z_0)$ is the Euclidean distance between a region with

location z_0 and the training region with location z_i , and the exponent q is set to 2. The exponent q in this formula controls the influence of near neighbors of z_0 in determining $\delta_g^{MID}(z_0)$. The choice of $q = 2$ as the exponent in the equation has the appeal of relating the MID classifier to the standard inverse square law. The effect of this classifier can be visualized by imagining the training data to be lights of equal intensity spread across the study area, and $\delta_g^{MID}(z_0)$ to be thought of as the average illumination generated by the lights of group G_g at z_0 (Steele, 2000). As the distance increases between training samples and unlabeled regions, the effect of the MID classifier decreases, i.e. the lights get dimmer. Thus, the closer and, if you will, brighter areas would then have higher probabilities of coertype membership than more distant and thus darker areas. The probability of membership in coertype g is estimated by:

$$P_g^{MID}(z_0) = \frac{\delta_g^{MID}(z_0)}{\sum_{k=1}^c \delta_k^{MID}(z_0)}.$$

Where $\sum_{k=1}^c \delta_k^{MID}(z_0)$ is the sum of the inverse distances between all training regions, regardless of coertype, and the region with location z_0 . While not especially accurate when taken alone, as it is based purely upon spatial configurations, the accuracies of Euclidean distance classifiers are significantly improved when combined with the MID spatial classifier using the product rule (Steele, 2000). In essence the MID classifier increases the probability that unlabeled regions close to training regions will be classified

as the training regions coertype, however, when the unlabeled regions are very distant from a training sample the influence of the MID classifier approaches zero (Steele, 2000).

Product rule

Suppose that two classifiers have produced membership probability estimates denoted by: $P_g^{UED}(x_0)$ and $P_g^{MID}(x_0)$, $g = 1, \dots, c$. Where $P_g^{UED}(x_0)$ is the probability that region x_0 belongs to coertype g according to the UED classifier and $P_g^{MID}(x_0)$ is the probability that region x_0 belongs to coertype g according to the MID classifier. The product rule (Steele, 2000) combines these two estimates by computing their relative products:

$$P_g^{prod}(x_0) = \frac{P_g^{UED}(x_0) P_g^{MID}(x_0)}{\sum_{j=1}^c P_j^{UED}(x_0) P_j^{MID}(x_0)}, g = 1, \dots, c.$$

In this case region x_0 is then assigned to coertype g if $P_g^{prod}(x_0)$ is the largest among $P_1^{prod}(x_0), \dots, P_c^{prod}(x_0)$.

The rule imposed a consensus agreement between the classifiers because, if any classifier predicts a probability of coertype membership near zero, then the relative product of the classifiers will also be near zero. Thus, if any classifier indicates that a region's membership in a particular coertype is unlikely, then the combination classifier is unlikely to label the region with that coertype (Steele, 2000). When assigning coertype labels to unlabeled regions, the probabilities for membership in each coertype

are calculated. The region is then labeled according to the covertype that produces the highest relative probability of membership.

Accuracy Assessment

Accuracy assessment is arguably the most important aspect of a classification. Therefore, it is imperative that it be undertaken with extreme care. The most objective and scientifically valid method of accuracy assessment would be to take a stratified random sample of classified regions and verify their covertypes in the field. However because I worked with historical data (1991, 1993, and 1995), a field survey was not possible. Therefore I relied upon the existing survey data and classification results to compute (1) the raw observed (surveyed) and predicted (classified) acreages, (2) a leave-one-out cross-validation assessment (McLachlan, 1992), and (3) an overlay analysis. The raw observed and predicted acreages provided a quick estimate of commission and omission errors, while the cross-validation and overlay analyses provided much more detailed assessments of classification performance.

Leave-One-Out Cross-Validation Accuracy Assessment

A leave-one-out cross-validation accuracy assessment was calculated by removing a single training region from the training sample, constructing the classification rule from this reduced training set, and then applying this new rule to classify the left out region. This process was repeated until each training region had been held out and classified once. These results were then used to calculate omission error and commission error. Omission error is the number of training regions incorrectly classified divided by

the total number of training regions for that class. It represents the percentage of training regions for each covertype that were misclassified, i.e. under-classification. Commission error is the number of training regions incorrectly classified divided by the total number of regions predicted to be in that covertype. Sometimes referred to as reliability, commission error represents the percentage of regions classified on a map that do not represent that category on the ground, i.e. over-classification.

Overlay Analysis

Overlay analysis used the PDC survey data in conjunction with the classification results to determine how much of the surveyed area was correctly identified. Overlay analysis involved converting the survey data and classification results into ArcInfo grids and then mathematically adding these grids together to produce combination grids. The key to getting useful combination grids was assigning the input grids initial values in a binary fashion. This means that the input grids had values in the pattern of 2^n where $n = 0, 1, 2, 3 \dots n$, because any natural integer can be expressed by the addition of a unique set of base 2 outcomes. I set all the survey grids so that UP had a value of 0 and PDCs had a value of 1. For the bi-variate classification results I set the value for UP to 0, and PDCs to 2. When these grids were then added together they produced unique values depending upon the values assigned to the areas of intersection. For the bi-variate combinations the resulting grid had values ranging from 0-3, with 0 being UP, 1 representing areas of omission, 2 representing areas of commission, and 3 representing areas of agreement, i.e. correctly classified. The overlay analysis for the tri-variate classifications followed the same technique but extended from an initial 5 classes instead

of 3: UP (0), surveyed PDC (1), surveyed IPDC (2), classified PDC (4), and classified IPDC (8), resulting in 16 unique values (0-15) in the combination grid.

The GIS data used during these analyses included: the final classified grids for each image date and type of classification, the PDC survey data provided by the BIA, BLM, and CMR collected in 1988, 1993, and 1995, and the current ownership layer from the Montana Natural Resource Information System (<http://nris.state.mt.us>). All of the GIS data were converted to the same Albers equal area projection prior to any processing.

Because sylvatic plague initially struck in 1992, and I wanted to get a good representation of the pre-plague conditions, I began with a 1991 image even though the only survey data, and thus training data, available prior to the plague infestation was from 1988. This was necessary in part because a suitable cloud free image was unavailable, and also because I was able to classify, by beginning with a 1991 image, a series of images 2 years apart to monitor change.

The 1988 field survey data were gathered using visual estimates of PDC boundaries, which were then delineated on 7.5 minute (1:24k scale) quad maps. Beginning in 1993 the survey data were collected using GPS. The 1993 survey is probably the most complete of any of the three years because it was the first survey performed after the plague outbreak was discovered. Thus, extra care was taken to ensure that all known PDCs were surveyed regardless of land ownership or stewardship. The 1995 survey is similarly complete except on BLM lands. Because of budget and personnel constraints, the BLM lands were divided into three proportional units and surveyed on a 3-year rotating basis, 1/3 in 1995, 1/3 in 1996, and 1/3 in 1997. Therefore, the BLM's acreage for 1995 represents approximately 1/3 of their existing PDCs, and I

did not feel comfortable including 1996 and 1997 data for training the 1995 image. Therefore, the cross-validation accuracy assessment results, which are derived directly from known covertime and locations, are most reliable, but the results of the other accuracy analyses are still important for understanding the nature of the errors that occurred.

Results

Bi-Variate Classifications

The total predicted area of PDCs remained very stable in the study area, rising slightly from 66,530 acres in 1991 to 67,958 in 1995 (Table 1). This stability was observed despite a 63.4% reduction in the area of PDCs mapped by surveys between 1988 (44,079 acres) and 1995 (16,149 acres). These comparative results suggest an over-classification of more than 20,000 acres in 1991, 30,000 in 1993, and 50,000 in 1995 (Table 1). Because I wanted to determine if there were differences in the proportions of error on lands managed by different government agencies and private landowners, i.e. stewardship classes, I calculated the difference densities (DD) for each stewardship class by taking the absolute differences between the observed (surveyed) and predicted (classified) acres of PDCs under that stewardship, and dividing this by the observed PDC acreages under that stewardship: $DD = \frac{|o - p|}{o}$ where o = observed acreages and p = predicted acreages. The results showed consistently lower differences in the CMR and consistently higher ones on private lands (Table 1). It is also worth noting that for all stewardships, aside from the Bureau of Reclamation (BOR) whose acreage was relatively

insignificant, the DD rose as the plague infestation spread between 1991 and 1995

(Table1).

Table 1. Relationships between land stewardship and the number of acres of PDCs observed vs. predicted for the bi-variate classifications.

Stewardship	Acres	% of SA ¹	Status	PDC Acres		
				1991	1993	1995
BIA	484,102	24.6	Observed	16,204	14,979	7,261
			Predicted	26,403	33,773	25,845
			DD ²	.63	1.25	2.56
BLM ³	66,889	3.4	Observed	11,685	5,969	2,772
			Predicted	17,189	12,143	15,547
			DD ²	.47	1.03	4.61
BOR	7,646	.4	Observed	27	69	0
			Predicted	143	136	24
			DD ²	4.29	.97	-
CMR	537,264	27.3	Observed	6,717	3,325	4,048
			Predicted	6,706	4,163	6,096
			DD ²	.001	.25	.51
Private	741,438	37.6	Observed	5,965	4,337	1,057
			Predicted	11,150	23,228	15,323
			DD ²	.87	4.36	13.5
State	132,763	6.7	Observed	3,468	2,653	1,011
			Predicted	4,939	5,042	5,123
			DD ²	.42	.9	4.08
Total	1,970,102	100	Observed	44,079	31,332	16,149
			Predicted	66,530	68,485	67,958
			Average DD ²	.51	1.19	3.21

1. SA = Study Area

2. DD = Difference Density

3. In 1995 approximately only 1/3 of BLM PDCs were surveyed, the observed BLM values are estimated.

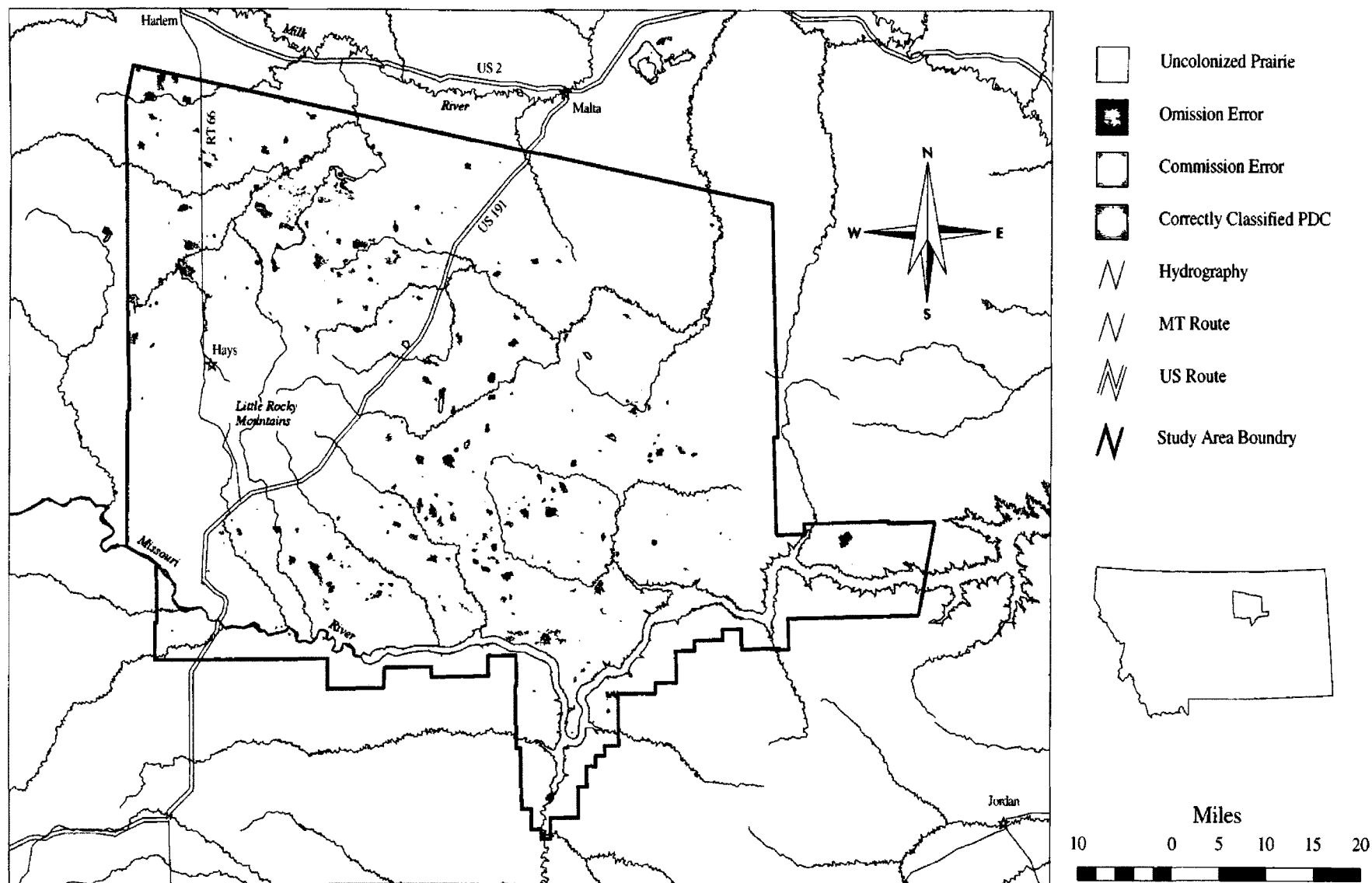


Figure 10. 1991 Bi-variate Classification Results.

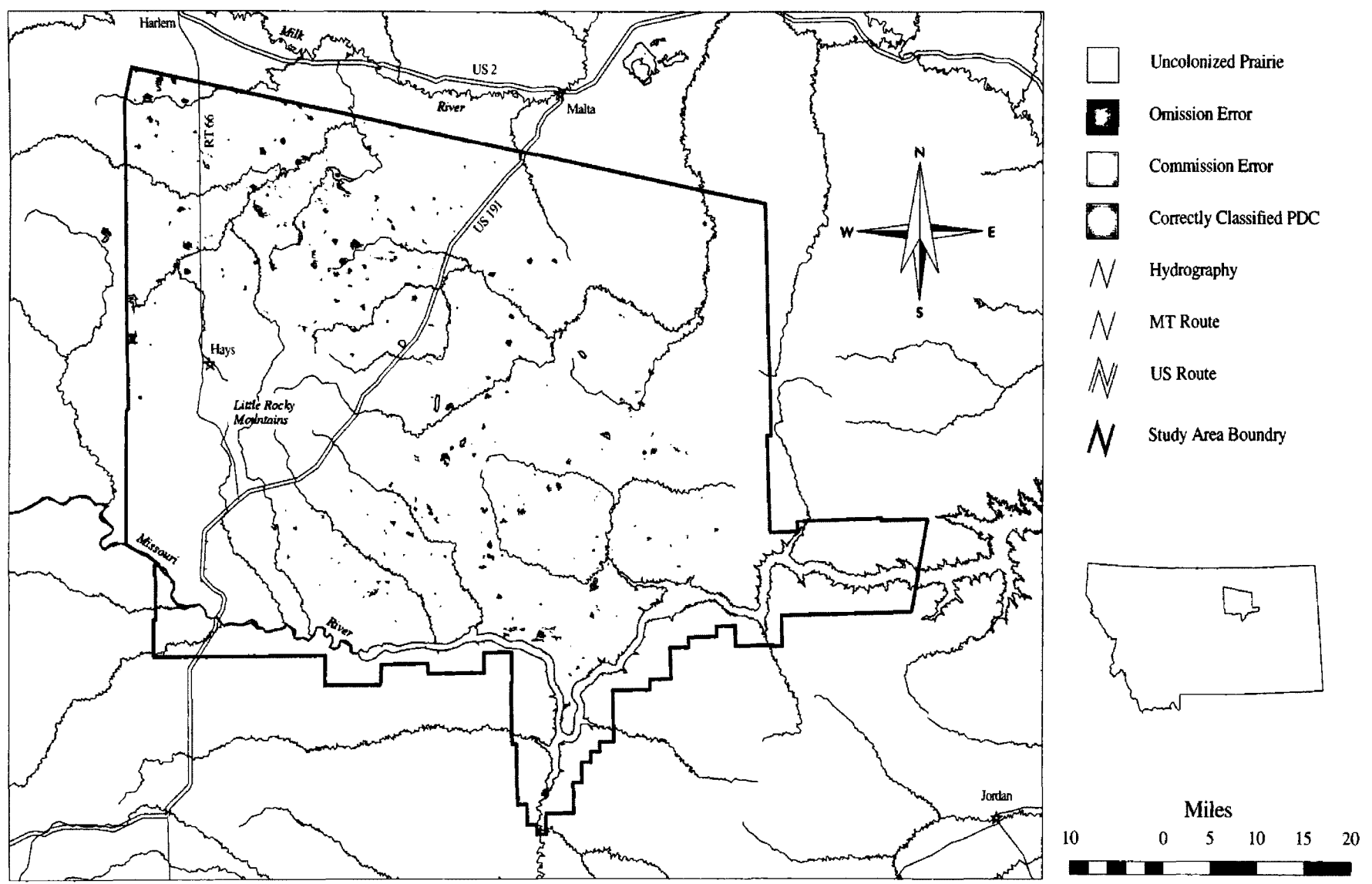


Figure 11. 1993 Bi-variate Classification Results.

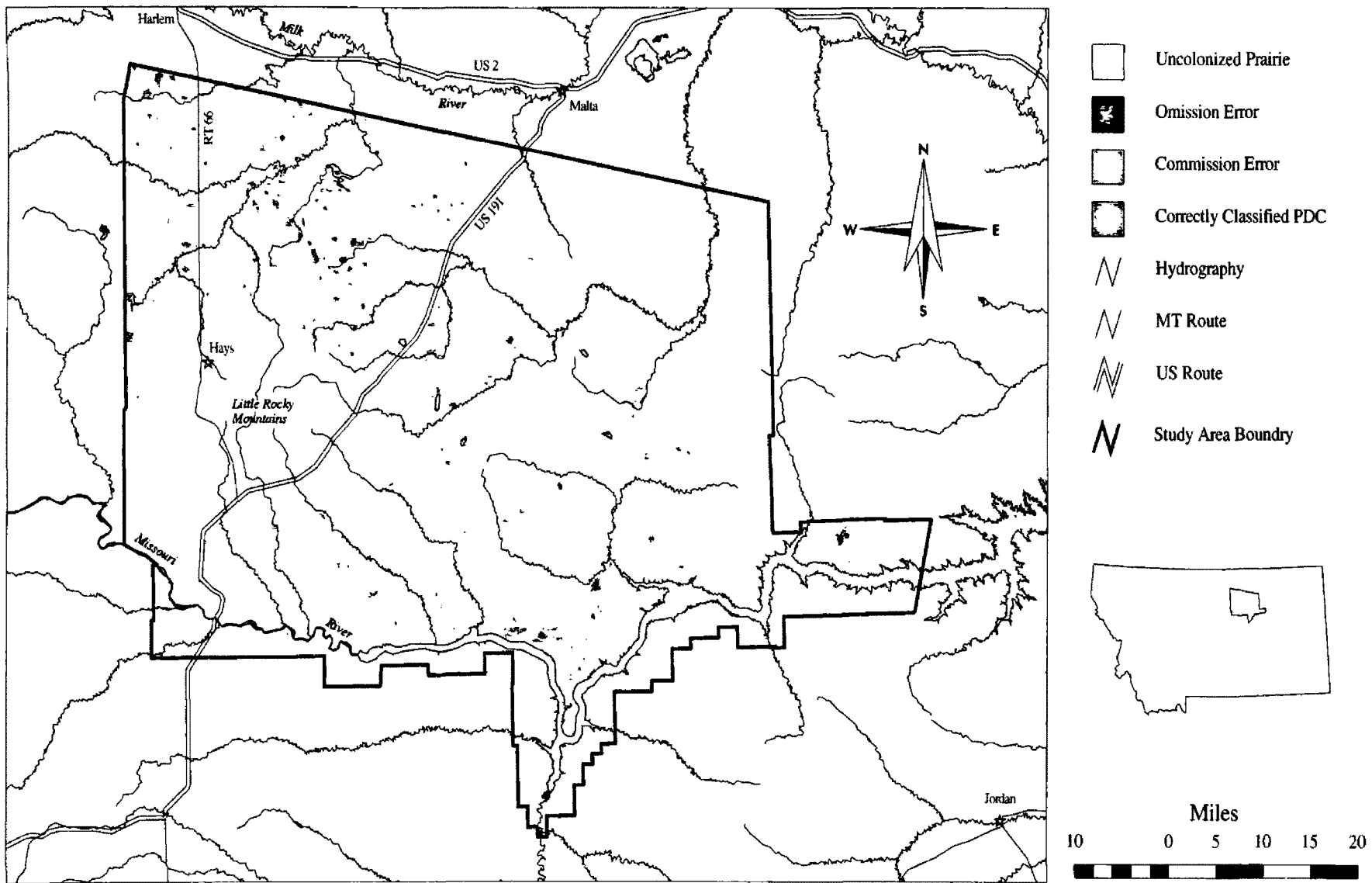


Figure 12. 1995 Bi-variate Classification Results.

Accuracy Assessments

My findings indicate that for the 1991 classification 22.4% of all PDC training regions were incorrectly classified. In 1993 this dropped to a low of 16.4%, and in 1995 went back up to 22.3% (Table 2). The omission errors derived from the overlay analyses were higher in 1991, very similar to observed in 1993 (17.1%), and significantly lower in 1995 (13.0%) (Table 3). Commission errors derived from cross validation stayed near 20% in all three years (Table 2). But the commission errors from the overlay analysis rose from 52% in 1991 to nearly 82% in 1995 (Table 3).

Table 2: Leave-one-out cross-validation statistics for the bi-variate classifications.

Predicted Covertypes	Observed Covertypes			Omission Error
	UP	PDC	Total TR¹	
1991				
Uncolonized Prairie	4902	98	5000	2%
Prairie Dog Colony	112	388	500	22.4%
Total TR Classified	5014	486	5500	Overall Error
Commission Error	2.3%	20.2%		3.8%
1993				
Uncolonized Prairie	4891	109	5000	2.2%
Prairie Dog Colony	82	418	500	16.4%
Total TR Classified	4973	527	5500	Overall Error
Commission Error	1.4%	20.7%		3.5%
1995				
Uncolonized Prairie	3361	84	3445	2.4%
Prairie Dog Colony	82	286	368	22.3%
Total TR Classified	3443	370	3813	Overall Error
Commission Error	2.4%	22.7%		4.4%

1. TR = Training Regions.

Table 3: Results of the bi-variate classifications overlay analyses showing the proportions of each error type and correctly classified areas.

Bi-variate Classifications			
1991 PDC	Overlay Acres¹	Total Acres	% Of Total
Omission Error	12,165	44,079 ²	27.6% of Surveyed Area
Commission Error	34,616	66,530 ³	52.0% of Predicted Area
Correct	31,914	44,079 ²	72.4% of Surveyed Area
		66,530 ³	48.0% of Predicted Area
1993 PDC			
Omission Error	5,352	31,332 ²	17.1% of Surveyed Area
Commission Error	42,505	68,485 ³	62.1% of Predicted Area
Correct	25,980	31,332 ²	82.9% of Surveyed Area
		68,485 ³	37.9% of Predicted Area
1995 PDC⁴			
Omission Error	1,852	14,301 ²	13.0% of Surveyed Area
Commission Error	55,510	67,959 ³	81.7% of Predicted Area
Correct	12,449	14,301 ²	87.0% of Surveyed Area
		67,959 ³	18.3% of Predicted Area

1. The areas of the regions produced by the overlay analysis.
2. The total area of surveyed PDCs in my study area.
3. The total area predicted to be PDCs by the classification.
4. In 1995 approximately only 1/3 of BLM PDCs were surveyed; these values are estimated.

Omission Error Analysis

Between 27-30% of all PDCs surveyed between 1988 and 1995 were missed by the supervised classifications (Table 4). The size of those colonies averaged 5-16 acres during the three time periods and made up only 3-4% of the total area of PDCs surveyed. The colonies that were partially predicted/missed averaged between 53 and 167 acres, and in addition, 72-87% of the areas of those colonies were correctly classified as PDCs.

Table 4: Results of the omission error analyses for the bi-variate classifications identifying the number and acreages of colonies that were missed or partially predicted/missed.

		Missed	Part Predicted	Part Missed	Total
1991	# PDCs	112 (30%)	253 (70%)		365
	Acres	1,805 (4%)	31,914 (72%)	10,361 (24%)	44,081
	Avg. Size	16	167		121
1993	# PDCs	114 (27%)	310 (73%)		424
	Acres	1,004 (3%)	25,980 (83%)	4,348 (14%)	31,332
	Avg. size	8.8	98		74
1995	# PDCs	95 (27%)	261 (72%)		356
	Acres	453 (3%)	12,449 (87%)	1,399 (10%)	14,302
	Avg. Size	5	53		40

Commission Error Analysis

To determine the extent to which IPDCs were being confused with PDCs, I performed another overlay analysis using the surveyed IPDCs and the PDC commission areas from the original overlay analysis. In 1993, 25.2%, or more than 5,000 acres of the surveyed IPDCs, were misclassified as PDCs, accounting for 12.4% of the total commission error (Table 5). In 1995, 48.5%, or more than 17,500 acres of the surveyed IPDCs, were classified as PDCs, accounting for 31.7% of the total commission error.

Table 5: Results of the commission error analysis comparing PDC commission and IPDCs.

1993	Overlay Acres¹	Total Acres	% Of Total
Surveyed IPDC	15,659	20,947 ²	74.8% of surveyed IPDC
PDC Commission	37,217	42,505 ³	87.6% of PDC Commission
IPDC Classified as PDC	5,288	20,947 ²	25.2% of surveyed IPDC
		42,505 ³	12.4% of PDC Commission
1995			
Surveyed IPDC	21,653	36,241 ²	59.7% of surveyed IPDC
PDC Commission	37,921	55,509 ³	68.3% of PDC Commission
IPDC Classified as PDC	17,588	36,241 ²	48.5% of surveyed IPDC
		55,509 ³	31.7% of PDC Commission

1. The areas of the regions produced by the overlay analysis.
2. The total surveyed IPDC area.
3. The total predicted IPDC area in the tertiary classifications.

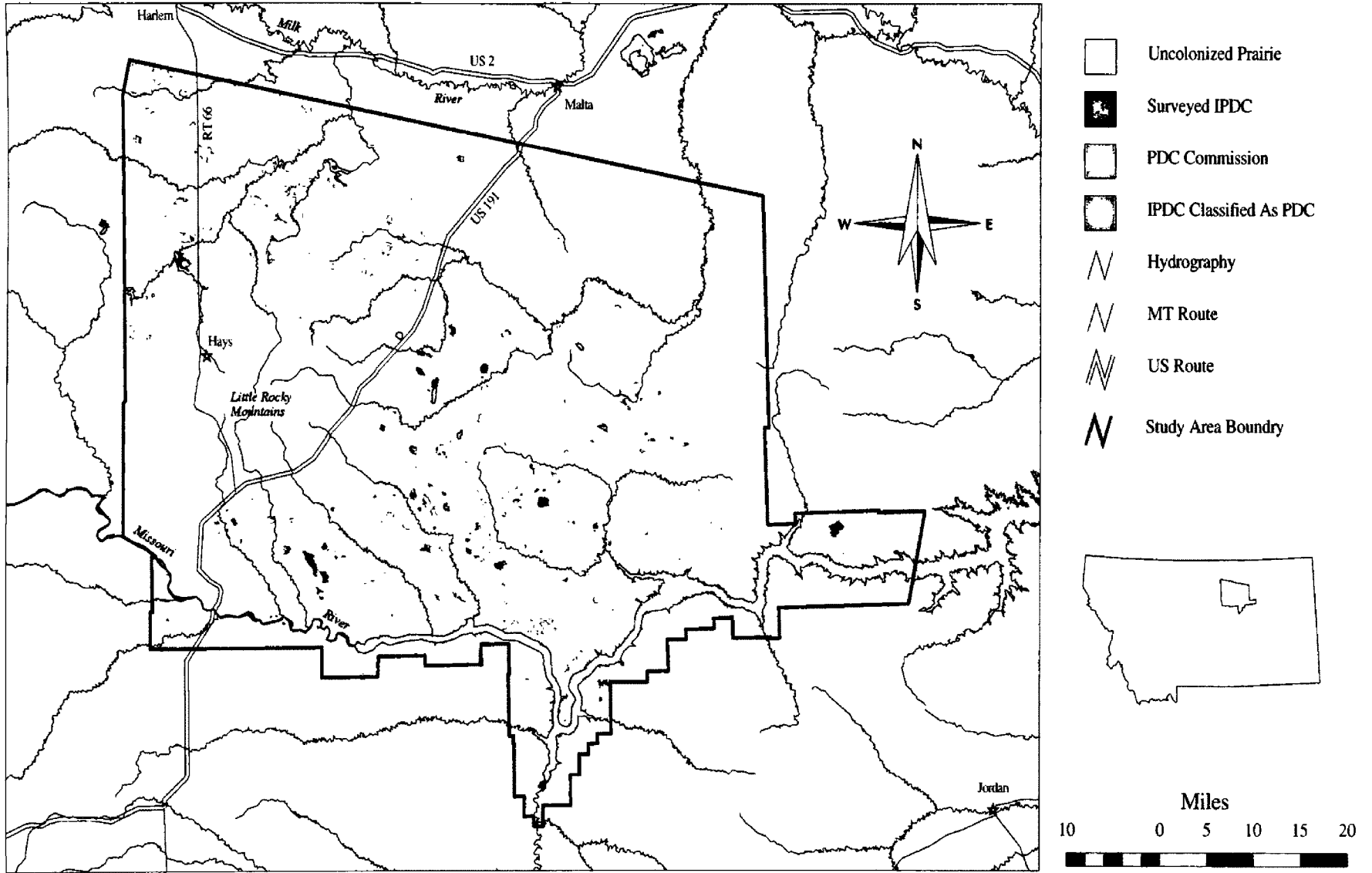


Figure 13. 1993 Bi-variate Commission Analysis Results.

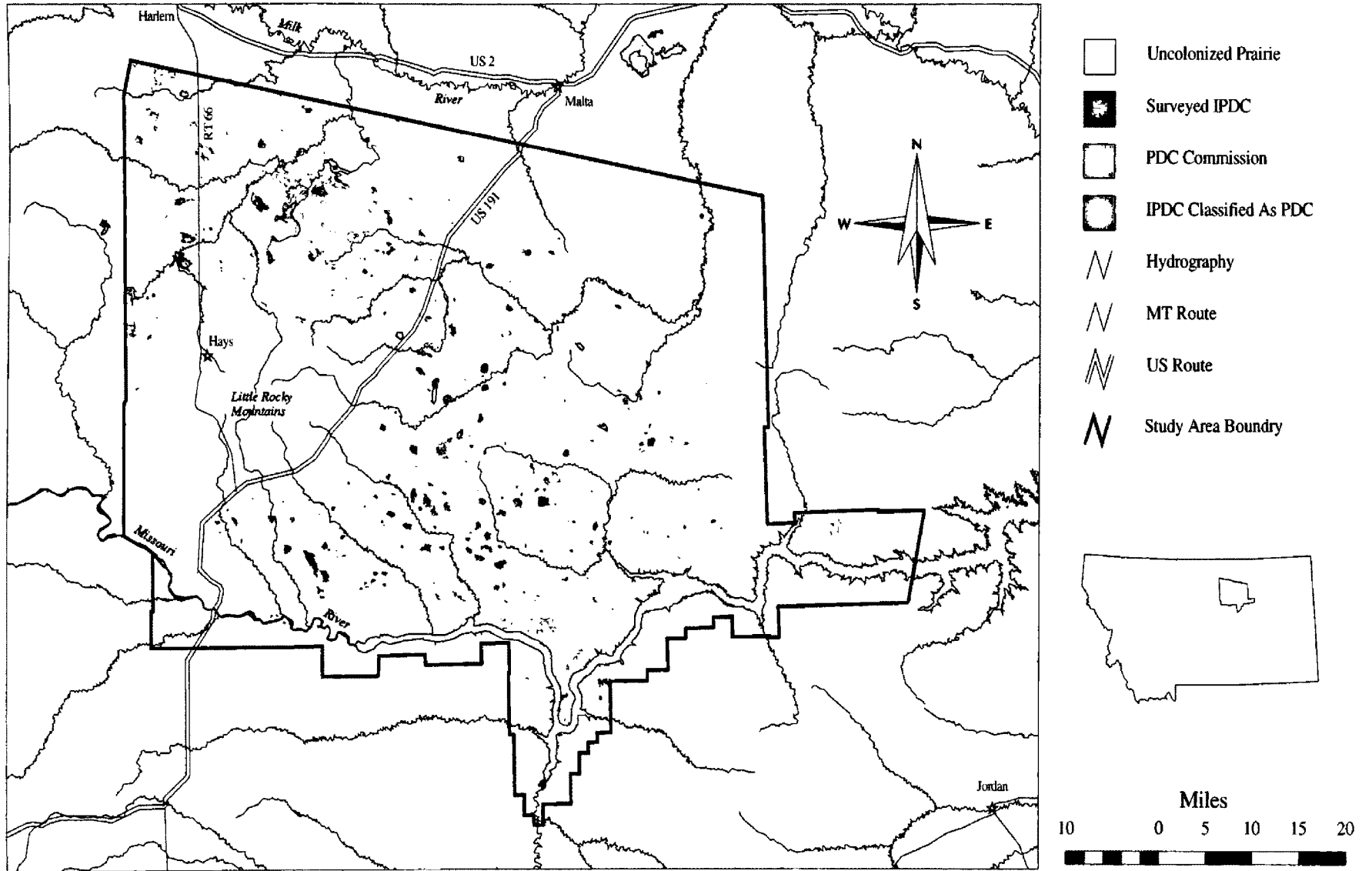


Figure 14. 1995 Bi-variate Commission Analysis Results.

Tri-Variate Classifications

Between 1993 and 1995 the tri-variate classifications predicted a net decrease of almost 10,000 acres in the PDC coertype and a 9,000 acre net increase in the IPDC coertype (Table 6). But the predicted acreages for both classes were considerably more than the acreages actually mapped each year. For example, the tri-variate classifications appeared to over predict PDCs by more than 30,000 acres in 1993 and 39,000 acres in 1995 (Table6). Similarly the IPDC coertype was over predicted by 17,000 acres in 1993 and dropping to less than 7,500 acres 1995 (Table 6). The difference densities for the PDC coertype were slightly lower than in the bi-variate classifications; however, in 1995 the DDs for the IPDC coertype were much lower than the PDCs' DDs in the bi-variate classifications. (Table 6).

Table 6: Relationship between the surveyed and predicted acreages of each coertype for the tri-variate classifications.

Status	Acres	
	1993	1995*
Observed PDC	31,332	14,302
Predicted PDC	63,045	53,237
Average DD	1.01	2.72
Observed IPDC	20,947	39,241
Predicted IPDC	37,896	46,703
Average DD	.81	.19

*In 1995 approximately only 1/3 of BLM PDCs were surveyed; these values are estimated.

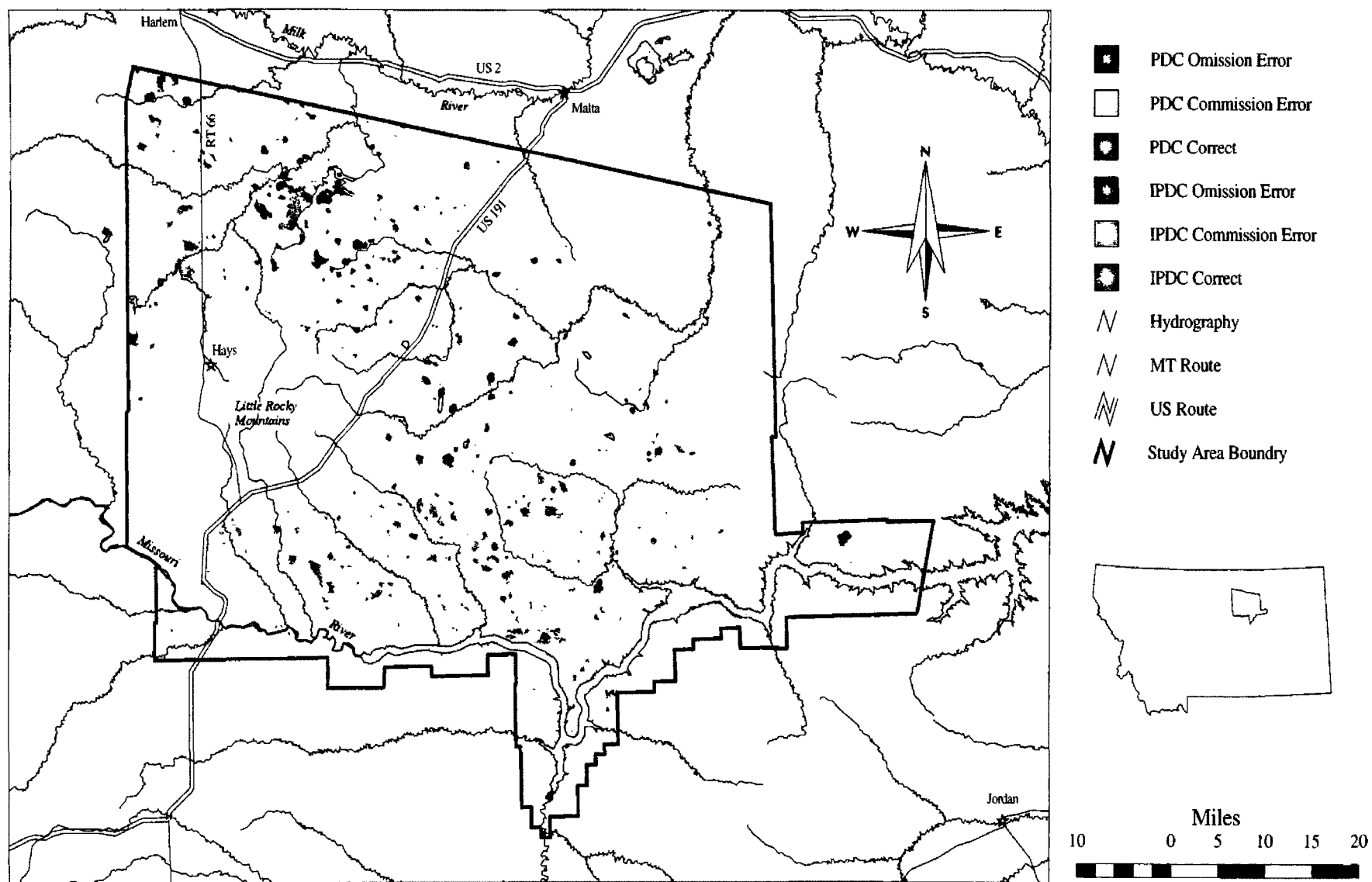


Figure 15. 1993 Tri-variate Classification Results.

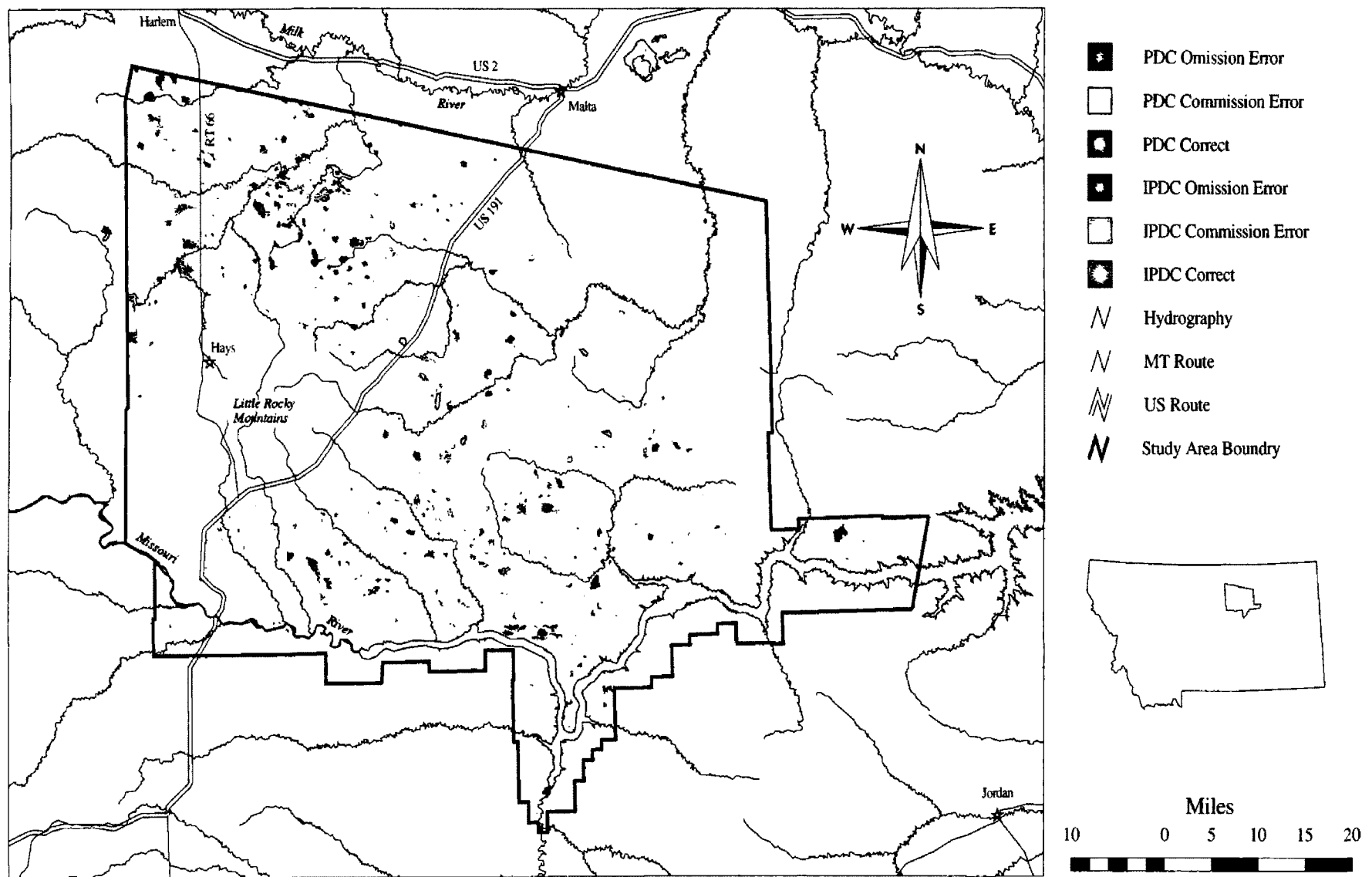


Figure 16. 1995 Tri-variate Classification Results.

Accuracy Assessments

Based on the leave-one-out cross-validation analysis, in 1993 25.6% of all training regions originally labeled as PDC for 1993 were incorrectly classified (Table 7). For 1995 the PDC omission error rose to 37%. Both of these rates are higher than those reported for the bi-variate classification's PDC coertype. The omission error for IPDCs began at 54.8% in 1993 and dropped to 42.6% in 1995 (Table 7). Almost half of the IPDC training regions were incorrectly classified. This is clearly an unacceptably high rate of error.

Commission error reported by cross-validation was also higher than those reported by the bi-variate classifications, especially for the IPDC coertype. In 1993 the commission error for the PDC coertype was 30% and it rose to 35.2% in 1995 (Table 7). The commission error for the IPDC coertype stayed fairly constant at 45-46% in both years. These again were much higher commission errors than those obtained from the bi-variate classifications.

Table 7: Leave-one-out cross-validation statistics for the tri-variate classifications.

1993	Original Covertypes				Omission Error
Predicted Covertypes	UP	IPDC	PDC	Total TR¹	
Uncolonized Prairie	4871	74	110	4965	1.9%
Inactive PDC	154	178	62	394	54.8%
Prairie Dog Colony	59	79	402	540	25.6%
Total TR Classified	4994	331	574	5899	Overall Error
Commission Error	2.5%	46.2%	30%		7.6%
1995					
Uncolonized Prairie	3296	78	71	3445	4.3%
Inactive PDC	90	195	55	340	42.6%
Prairie Dog Colony	54	82	232	368	37%
Total TR Classified	3440	355	358	4153	Overall Error
Commission Error	4.2%	45.1%	35.2%		10.4%

1. TR = Training Regions.

In 1993 according to the overlay analysis, only 54.9% of the surveyed IPDCs were correctly classified as IPDC, making up only 30.3% of the total predicted IPDC area (Table 8). By 1995 the correct classification of surveyed IPDC dropped to 39%, making up a total of 32.7% of the total predicted IPDC. With IPDC omission errors starting near 50% and increasing to over 61%, it is clear that the tri-variate classifications weren't working.

Table 8: The results of the tri-variate classifications overlay analyses.

Tri-variate Classifications			
1993 PDC	Overlay Acres¹	Total Acres	% Of Total
Omission Error	6,283	31,332 ²	20.1% of surveyed
Commission Error	37,896	62,945 ³	60.2% of classified
Correct	25,049	31,332 ²	79.9% of surveyed
		62,945 ³	39.8% of classified
1993 IPDC			
Omission Error	9,451	20,947 ²	45.1% of surveyed
Commission Error	26,400	37,896 ³	69.7% of classified
Correct	11,496	20,947 ²	54.9% of surveyed
		37,896 ³	30.3% of classified
1995 PDC⁴			
Omission Error	3,246	14,302 ²	22.7% of surveyed
Commission Error	42,181	53,237 ³	79.2% of classified
Correct	11,056	14,302 ²	77.3% of surveyed
		53,237 ³	20.8% of classified
1995 IPDC⁴			
Omission Error	23,945	39,240 ²	61.0% of surveyed
Commission Error	31,408	46,703 ³	67.3% of classified
Correct	15,295	39,240 ²	39.0% of surveyed
		46,703 ³	32.7% of classified

1. The areas of the regions produced by the overlay analysis.
2. The total area of surveyed PDCs or IPDCs in my study area.
3. The total area predicted to be PDCs or IPDCs by the tri-variate classifications.
4. In 1995 approximately only 1/3 of BLM PDCs were surveyed; these values are estimated.

Discussion

Bi-variate classifications

The bi-variate classifications were intended to test whether or not I could accurately predict the presence or absence of PDCs. Verification of the results in the field would be the best way to assess their accuracy; however, because I was working with historical data, field verification was impossible. Instead I had to rely on the survey data for accuracy assessment. Although these surveys were performed carefully, it is

unlikely that they recorded and accurately mapped every PDC in the study area. But unfortunately at this point in time there is no easy way to distinguish between the correct classification of undocumented PDCs and true commission errors.

As the plague spread and the amount of active PDCs surveyed decreased, my total predicted area of PDCs did not. Thus, commission errors rose significantly between 1993 and 1995. These commission errors could be due to the inclusion of undocumented PDCs in the classification, confusion between PDC and/or other similar covertypes, or both. In the commission error analysis I determined that 12.4% in 1991 and 31.7% in 1995 of these areas were made up of surveyed IPDCs that were being mistakenly classified as PDCs. In addition, with over 700,000 acres of private lands in the study area, many of which were unsurveyed for PDCs, and a predicted PDC acreage of between 11,000 and 23,000 acres, or 16.5 and 33.9% of the total predicted acreage of PDCs respectively, it is highly likely that some of this “commission error” can be attributed to the correct classification of undocumented PDCs. This assertion is also supported by the relatively high DDs on private lands.

Because of the tendency for the bi-variate classifications to over predict PDCs, one might expect relatively low commission errors. Yet both the cross-validation and overlay analyses indicated that between 16 and 28% of all PDCs surveyed between 1988 and 1995 were missed by the classifications (Tables 2 and 3). Fortunately though those colonies that were missed tended to be much smaller than the average; and made up just a small fraction of the overall PDC area.

Tri-variate Classifications

The purpose of the tri-variate classifications was to determine if inactive PDCs, due to plague or other factors, could be classified separately from active PDCs and uncolonized prairie. It became apparent fairly early that it was not working very well. The low accuracies recorded for the tri-variate classifications, as well as the lack of decline in total acreage identified as active PDCs in the bi-variate classifications over the course of the plague infestation, led me to conclude that either my methods and or data, as outlined above, were inadequate to accurately discern between inactive and active PDCs. This is understandable because IPDCs represent a continuum between active PDCs and uncolonized prairie. This wide range of spectral response makes it very difficult to define a distinct IPDC class.

Although classifying IPDC directly may not be feasible, IPDC can still be derived indirectly using a series of bi-variate classification results and overlay analysis, much in the same way I determined the surveyed IPDC areas from the PDC survey data. First one must assume that any PDCs from the previous years classification or survey represents active for that year. Then by overlaying subsequent years classifications it can be determined which of the previously classified areas were not classified in the subsequent year. These areas would be then labeled IPDCs in the new classification.

Conclusions

My research shows that PDCs can be mapped fairly accurately from Landsat TM imagery; however accurately distinguishing PDCs from IPDCs was not possible. The spatial resolution of 30 x 30 meters is quite adequate for the identification of PDCs, and

any higher resolution imagery would, in my opinion, create more problems than benefits by accentuating the significant variation within PDCs, and by creating a significantly more cumbersome dataset. The overall tendency of my classifications was to over predict PDCs and IPDCs, while consistently missing the very small, i.e. < 15 acre, colonies. Although commission errors were fairly high, a good percentage of these errors (12-32%) were due to confusion with IPDC.

One important and as yet unanswered question remains: what percentage of the commission areas were really undocumented active PDCs. It is clear that some of the commission error, particularly on private lands, is likely to represent active PDCs however I cannot say for what percentage this is true. Future research using current imagery and a post classification survey (see below) could answer this question, and in so doing provide further validation of the method as well as the basis for deciding whether to apply this methodology to other areas. If such validation were successful, it would greatly help promote and improve the management and conservation of prairie dogs and related species across western North America.

Future research

If I were to begin this project again I would begin by selecting a current TM image date and then carefully planning and executing a field survey designed explicitly to collect training data. This would enable the tailoring of survey design for more accurate feature representation, which would then be reflected by higher accuracies in the subsequent classifications. As part of the pre-processing I would perform a simple, 10-20 class, unsupervised classification and use this to mask out any covertypes not associated

with known PDCs. The image segmentation and supervised classifications could then be run, and the results assessed using cross validation analysis. These results would then be used to help design a post classification survey for the collection of field data to be used in an independent accuracy assessment. These changes would provide, in my opinion, a more accurate classification, and a sounder method of assessing its accuracy.

LITERATURE CITED

- Anderson, E., S.C. Forrest, T.W. Clark, and L. Richardson. 1986. Paleo-biology, biogeography, and systematics of the black-footed ferret, *Mustela nigripes*, Great Basin Naturalist Memoirs 8:11-62.
- Barsness, S. 1996. Aggregating raster polygons derived from large remotely sensed images. Unpublished M.S. Thesis, The University of Montana, Missoula. 58pp.
- Biggens, D., B. Miller, L. R. Hanebury, B. Oakleaf, A.H. Farmer, R. Crete, and A. Dood. 1993. A system for evaluating black-footed ferret habitat. Pp. 73-92 in Proceedings of the Symposium on the Management of Prairie Dog Complexes for the Reintroduction of the Black-footed Ferret, John Jones ed. U.S. Fish and Wildlife Service Biological Report 13. US Government Printing Office, Washington, D. C.
- Cid, M.S., J. K. Detling, A.D. Whicker, and M.A. Brizuela. 1991. Vegetational responses of a mixed-grass prairie site following exclusion of prairie dogs and bison, Journal of Range Management, 44 (2): 100-105.
- Clark, T.W., D. Hinckley, and T. Rich. 1989. The prairie dog ecosystem: Managing for biodiversity, Montana BLM Wildlife Technical Bulletin No. 2.
- Clippinger, N.W. 1989. Habitat Suitability Index Models: black-tailed prairie dog, U.S. Fish and Wildlife Service Biological Report 82 (10.156).
- Congalton, R. G., 1988. A Comparison of Sampling Schemes Used in Generating Error Matrices for Assessing the Accuracy of Maps Generated from Remotely Sensed Data, Photogrammetric Engineering and Remote Sensing 54(5): 593-600.
- Coppock, D.L., J.K. Detling, J.E. Ellis, and M.I. Dyer. 1983. Plant-Herbivore Interactions in a North American Mixed-Grass Prairie, Oecologia 1983 56:1-9.
- ERDAS, 1997. Field Guide, Fourth Edition, ERDAS, Atlanta Georgia, 656pp.
- Foster, N. S., and S.E. Hygnstrom. 1990. Prairie Dogs and Their Ecosystem, University of Nebraska-Lincoln, Department of Forestry, Fisheries and Wildlife. Lincoln, Nebraska, 8pp.
- Hogg, J.T., N.S. Weaver, J.J. Craighead, B.M. Steele, M.L. Pokorny, M.H. Mahr, R.L. Redmond, and F.B. Fisher. 2001. Vegetation patterns in the Salmon-Selway ecosystem: an improved land cover classification using Landsat TM imagery and wilderness botanical surveys. Craighead Wildlife-Wildlands Institute Monograph number 2, Missoula, MT. 98 pp.

- Jensen, J.R. 1996. *Introductory Digital Image Processing A Remote Sensing Perspective*, Second Edition, Prentice Hall, Upper Saddle River, N.J., 318pp.
- Lillesand, T.M., and R. W. Kieffer, 1994. *Remote Sensing and Image Interpretation*, Third Edition, John Wiley and Sons, New York, N.Y., 721pp.
- Ma, Zhenkui, M. Hart, and R.L. Redmond. 2001. Mapping Vegetation Across Large Geographic Areas: Integration of Remote Sensing and GIS to Classify Multisource Data. *Photogrammetric Engineering and Remote Sensing* 67(3): 295-307.
- Marsh, R.E. 1984. Ground squirrels, prairie dogs and marmots as pests on rangeland. Pp. 195-208 in *Proceedings of the conference for organization and practice of vertebrate pest control*, Hampshire England.
- McLachlan, Geoffrey J., 1992. *Discriminant Analysis and Statistical Pattern Recognition*. John Wiley and Sons, New York, N.Y., 526 pp.
- Miller, B., G. Ceballos, and R.P. Reading. 1994. The Prairie Dog and Biotic Diversity. *Conservation Biology* 8(3): 677-681.
- Nemani, R., L. Pierce, S. Running, and S Band, 1993. Forest Ecosystem Processes at the Watershed Scale: Sensitivity to Remotely Sensed Leaf Area Index Estimates. *International Journal of Remote Sensing* 14(13): 2519-2534.
- Oldmeyer, John L., D.E. Biggins, and B.J. Miller. 1993. *Proceedings of the Symposium on the Management of Prairie Dog Complexes for the Reintroduction of the Black-footed Ferret*. U.S. Fish and Wildlife Service Biological Report 13. US Government Printing Office, Washington, D. C.
- Proctor, John 1998. *A GIS Model for Identifying Potential Black-tailed Prairie Dog Habitat in the Northern Great Plains Shortgrass Prairie*. Unpublished M.S. Thesis, The University of Montana, Missoula. 56pp.
- Reading, R. P., and R. Matchett. 1997. Attributes of Black-tailed Prairie Dog Colonies in Northcentral Montana. *Journal of Wildlife Management* 61(3): 664-673.
- Sharps, J., and D. Uresk. 1990. Ecological review of Black-tailed prairie dogs and associated species in western South Dakota. *Great Basin Naturalist* 50: 339-345.
- Steele, B.M. 2000. Combining Multiple Classifiers: An Application Using Spatial and Remotely Sensed Information for Land Cover Type Mapping. *Remote Sensing of Environment* 74:545-556.

- Steele, B.M., J.C. Winne, and R.L. Redmond. 1998. Estimation and Mapping of Misclassification Probabilities for Thematic Land Cover Maps. *Remote Sensing of the Environment* 66:192-202.
- Steele, B. M. and R.L. Redmond. 2001 A method of exploiting spatial information for improving classification rules: An Application to the construction of polygon-based landcover maps. *International Journal of Remote Sensing* 22: 3143-3166.
- Steele, B.M. and D.A. Patterson. 2001. Land Cover Mapping Using Combination and Ensemble Classifiers. in *Proceedings of the 33rd Symposium on the Interface*. Interface Foundation of North America. In Press.
- Steele, B.M, D.A. Patterson, and R.L. Redmond. 2002. Toward the estimation of map accuracy without a probability test sample. *Environmental and Ecological Statistics*. In Press.
- Uresk, D. W., 1985. Effects of Controlling Black-tailed Prairie Dogs on Plant Production. *Journal of Range Management* 38(5): 466-468.
- Uresk, D. W. and D.B. Paulson. 1989. Estimated carrying capacity for cattle competing with prairie dogs and forage utilization in western South Dakota. Pp. 287-290 in *Symposium on Management of Amphibians, Reptiles, and Small Mammals in North America*, R. C. Szaro, K. E. Severson, and D. R. Patton eds. U.S. Forest Service General Technical Report RM-166. Washington, DC: U.S. Forest Service.

APPENDICES

Appendix 1: 1991 Bi-variate Data.

Overall Acreages	Pixel Count	Acres
Surveyed PDCs	198203	44079.33
Classified PDCs	299153	66530.09
Overlay Analysis Results		
PDC Omission	54703	12165.67
PDC Commission	155653	34616.43
Correctly Classified	143500	31913.66
Surveyed PDC Stewardship		
BIA	72861	16203.91
BLM	52542	11685.07
BOR	122	27.13
CMR	30203	6716.99
Private	26882	5965.07
State	15593	3467.8
Predicted PDC Stewardship		
BIA	118721	26402.94
BLM	77291	17189.12
BOR	644	143.22
CMR	30152	6705.65
Private	50138	11150.43
State	22207	4938.72

Cross Validation Results	Observed Coverture			% Omission Error
Predicted Coverture	UP	PDC	Total TR¹	
UP Classified	4902	98	5000	2
PDC Classified	112	388	500	22.4
Total # Classified	5014	486	5500	
% Commission Error	2.3	20.2		

1. TR = Training Regions.

Appendix 2: 1993 Bi-variate Data.

Overall Acreages	Pixel Count	Acres
Surveyed PDCs	140885	31332.1
Classified PDCs	307943	68484.94
Overlay Analysis Results		
PDC Omission	24067	5352.38
PDC Commission	191125	42505.22
Correctly Classified	116818	25979.72
Surveyed PDC Stewardship		
BIA	67353	14978.96
BLM	26840	5969.08
BOR	310	68.94
CMR	14953	3325.47
Private	19500	4336.7
State	11929	2652.95
Predicted PDC Stewardship		
BIA	151860	33772.88
BLM	54600	12142.76
BOR	612	136.11
CMR	18719	4163.01
Private	59479	13227.82
State	22673	5042.36
Commission Analysis Results		
Surveyed IPDC	70411	15659.04
PDC Commission	167348	37217.34
Area in Agreement	23777	5287.88

Cross Validation Results	Observed Covertypes			% Omission Error
Predicted Covertypes	UP	PDC	Total TR¹	
Uncolonized Prairie	4891	109	5000	2.2
Prairie Dog Colony	82	418	500	16.4
Total TR Classified	4973	527	5500	
% Commission Error	1.4	20.7		

1. TR = Training Regions.

Appendix 3: 1993 Tri-variate Data.

Overall Acreages	Pixel Count	Acres
Surveyed PDCs	140885	31332.1
Predicted PDCs	283483	63045.16
Surveyed IPDCs	94188	20946.93
Predicted IPDCs	170398	37895.64
Overlay Analysis Results		
PDC Omission	28250	6282.65
PDC Commission	170848	37995.72
PDC Correctly Classified	112635	25049.45
IPDC Omission	42498	9451.34
IPDC Commission	118708	26400.05
IPDC Correctly Classified	51690	11495.59

Cross Validation Results	Original Covertypes				% Omission Error
	UP	IPDC	PDC	Total TR¹	
Predicted Covertypes					
Uncolonized Prairie	4871	74	110	4965	1.9
Inactive PDC	154	178	62	394	54.8
Prairie Dog Colony	59	79	402	540	25.6
Total TR Classified	4994	331	574	5899	
% Commission Error	2.5	46.2	30		

1. TR = Training Regions.

Appendix 4: 1995 Bi-variate Data.

Overall Acreages	Pixel Count	Acres
Surveyed PDCs	64308	14301.77
Predicted PDCs	305578	67958.98
Overlay Analysis Results		
PDC Omission	8330	1852.55
PDC Commission	249600	55509.76
Correctly Classified	55978	12449.22
Stewardship		
Surveyed PDCs		
BIA	32647	7260.52
BLM	4155	924.05
BOR	0	
CMR	18203	4048.25
Private	4756	1057.71
State	4547	1011.23
Predicted PDCs		
BIA	116214	25845.4
BLM	69909	15547.4
BOR	109	24.24
CMR	27412	6096.29
Private	68899	15322.78
State	23035	5122.87
Commission Analysis Results		
Surveyed IPDC	97361	21652.59
PDC Commission	170514	37921.44
Area in Agreement	79086	17588.32

1995 Predicted Covertypes	Observed Covertypes			% Omission Error
	UP	PDC	Total TR¹	
Uncolonized Prairie	3361	84	3445	2.4
Prairie Dog Colony	82	286	368	22.3
Total TR Classified	3443	370	3813	
% Commission Error	2.4	22.7		

1. TR = Training Regions

Appendix 5: 1995 Tri-variate Data.

Overall Acreages	Pixel Count	Acres
Surveyed PDCs	64308	14301.77
Predicted PDCs	239379	53236.67
Surveyed IPDCs	176447	39240.9
Predicted IPDCs	210001	46703.14
Overlay Analysis Results		
PDC Omission	14594	3245.63
PDC Commission	189665	42180.52
PDC Correctly Classified	49714	11056.14
IPDC Omission	107671	23945.48
IPDC Commission	141225	31407.72
IPDC Correctly Classified	68776	15295.43

Cross Validation Results	Observed Covertypes				% Omission Error
	UP	IPDC	PDC	Total TR¹	
Predicted Covertypes					
Uncolonized Prairie	3296	78	71	3445	4.3
Inactive PDC	90	195	55	340	42.6
Prairie Dog Colony	54	82	232	368	37
Total TR Classified	3440	355	358	4153	
% Commission Error	4.2	45.1	35.2		

1. TR = Training Regions.